Phenylketonuria as a protein misfolding disease: The mutation pG46S in phenylalanine hydroxylase promotes self-association and fibril formation

João Leandro [a,b], Nina Simonsen [a], Jaakko Saraste [a], Paula Leandro [b], Torgeir Flatmark [a,*]

[a] Department of Biomedicine, University of Bergen, Jonas Lies vei 91, N-5009 Bergen, Norway
[b] Metabolism and Genetics Group, iMed.UL, Faculty of Pharmacy, University of Lisbon, Av. Prof. Gama Pinto, 1649-003 Lisbon, Portugal

ARTICLE INFO

ABSTRACT

The missense mutation pG46S in the regulatory (R) domain of human phenylalanine hydroxylase (hPAH), associated with a severe form of phenylketonuria, generates a misfolded protein which is rapidly degraded on expression in HEK293 cells. When overexpressed as a MBP-G46S fusion protein, soluble and fully active tetrameric/dimeric forms are assembled and recovered in a metastable conformational state. When MBP is cleaved off, G46S undergoes a conformational change and self-associates with a lag phase and an autocatalytic growth phase (tetramers $\gg$ dimers), as determined by light scattering. The self-association is controlled by pH, ionic strength, temperature, protein concentration and the phosphorylation state of Ser16; the net charge of the protein being a main modulator of the process. A superstoichiometric amount of WT dimers revealed a 2-fold enhancement of the rate of G46S dimer self-association. Electron microscopy demonstrates the formation of higher-order oligomers and linear polymers of variable length, partly as a branching network, and partly as individual long and twisted fibrils (diameter ~145–300 Å). The heat-shock proteins Hsp70/ Hsp40, Hsp90 and a proposed pharmacological PAH chaperone (3-amino-2-benzyl-7-nitro-4-(2-quinolyl)- 1,2-dihydroisoquinolin-1-one) partly inhibit the self-association process. Our data indicate that the G46S mutation results in a N-terminal extension of α-helix 1 which perturbs the wild-type α–β sandwich motif in the R-domain and promotes new intermolecular contacts, self-association and non-amyloid fibril formation. The metastable conformational state of G46S as a MBP fusion protein, and its self-association propensity when released from MBP, may represent a model system for the study of other hPAH missense mutations characterized by misfolded proteins.

© 2010 Elsevier B.V. All rights reserved.

1. Introduction

The human inborn error of metabolism phenylketonuria (PKU; OMIM# 261600) is caused by a dysfunction of the liver enzyme phenylalanine hydroxylase (hPAH; EC 1.14.16.1), inherited in an autosomal recessive fashion. At present > 500 disease causing mutations have been identified in the human *PAH* gene (see PAH Mutation Analysis Consortium database: http://www.pahdb.mcgill.ca/) [1]. Most of them are associated with PKU, and a smaller number has been identified among non-PKU hyperphenylalaninemia (HPA) patients. The current spectrum of alleged PKU/HPA mutations consists of ~60% missense substitutions, ~13% splice variants, ~13% deletions, ~6% nonsense (termination) mutations, and a few insertions, representing a broad spectrum of clinical, metabolic and enzymatic phenotypes [2]. Expression analyses of ~100 missense mutations in complementary in vitro systems (for review, see the PAH Mutation Analysis Consortium database) [1] have identified at least three main groups of enzymatic phenotypes which differ in their kinetic behavior and/or stability [3,4], i.e. (i) structurally stable mutations with altered kinetic properties, e.g. mutations at residues involved in substrate (L-phenylalanine, L-Phe) or the pterin cofactor ((6R)-L-*erythro*-5,6,7,8-tetrahydrobiopterin, BH$_4$) binding; (ii) mutations with normal or almost normal kinetic properties, but reduced stability both in vitro and in vivo; and (iii) mutations affecting both kinetic and stability properties of the enzyme.

Since a majority of the mutations results in enzyme forms with a propensity to self-associate when expressed as recombinant proteins in *E. coli* or in an in vitro transcription–translation system, PKU is often considered as a protein misfolding disease [5]. These mutations are located in different regions of the three-domain structure [4,6–9], and the mechanism of self-association may therefore have a variable structural basis. When overexpressed in *E. coli* several misfolding mutations result in both soluble and insoluble "aggregates", even when expressed and purified as MBP fusion proteins. Although MBP has been shown to have a chaperone like effect [10,11], the soluble mutant

proteins are often recovered mostly as higher-order oligomers [4,6,9]. However, in some mutations, e.g. the missense mutation pG46S in the regulatory (R) domain, the expressed protein is assembled and recovered as stable tetrameric/dimeric forms, in addition to some soluble higher-order oligomers [12]. The MBP-G46S-hPAH tetramer is characterized by a near normal catalytic efficiency, but when the tetramer is cleaved by the restriction protease factor Xa, the G46S tetramer is destabilized and self-associates [12]. When expressed in eukaryotic cells as a non-fusion protein the enzyme is unstable and is rapidly degraded [12], thus explaining the severe PKU phenotype. However, the molecular mechanism of the self-association and the structural properties of the higher-order oligomers remain to be determined.

In the present study, the pG46S mutation was carefully analyzed. This mutation belongs to the second group of enzymatic phenotypes previously defined, with reduced stability both *in vitro* and *in vivo* that results in a severe form of PKU [12]. This group represents a large proportion of the PKU mutations, with a loss-of-function pathogenesis due to reduce stability [13]. The mutation pG46S is also located in the regulatory domain of hPAH, and there is growing evidence that the R-domain of hPAH is largely involved in the instability of hPAH mutant proteins [9]. Therefore, the recombinant WT-hPAH and the G46S-hPAH mutant form were isolated as MBP-(pep)$_{Xa}$-PAH fusion proteins with the goal to: (i) characterize the self-association process of G46S-hPAH induced *in vitro* by factor Xa cleavage and how the solvent conditions affect its propensity to self-associate; (ii) examine the effect of substrates (L-Phe and BH$_4$), phosphorylation of Ser16 (Ser16 is, together with substrate and cofactor, one of the main regulators of hPAH function, involved in the activation of the enzyme [14] and causing conformational changes in the regulatory domain [15,16]) and molecular/pharmacological/chemical chaperones on the propensity to self-associate; (iii) investigate if the self-association results in the formation of any stable polymeric structures such as fibrils, and (iv) gain some insight into the molecular mechanism by which such structures are formed. To answer these questions, we used a combined approach of real-time light-scattering, thioflavin-T and ANS fluorescence and structural analyses by electron microscopy (EM). Additionally, complementary studies on a MBP fusion protein with the regulatory domain, comprising residues 2–120, were performed on the WT and G46S mutant form.

2. Material and methods

2.1. Materials

TB1 cells, the prokaryotic expression vector pMAL-c2/pMAL-hPAH and the amylose resin were obtained from New England Biolabs (USA). The restriction protease factor Xa was obtained from Protein Engineering Technology ApS (Aarhus, Denmark). The catalytic *C*-subunit of cAMP-dependent protein kinase (PKA) was from Biaffin GmBH & Co KG (Kassel, Germany). SDS molecular mass standard (low M_r range) was delivered by Bio-Rad. The pterin cofactor tetrahydrobiopterin (BH$_4$) was obtained from Schircks Laboratories (Jona, Switzerland) and glycerol, trimethylamine *N*-oxide (TMAO) and (−)-epigallocatechin gallate (EGCG) were from Sigma-Aldrich (St. Louis, MO, USA). 3-amino-2-benzyl-7-nitro-4-(2-quinolyl)-1,2-dihydroisoquinolin-1-one was purchased from Maybridge (Tintagel, Cornwall, UK). The recombinant human molecular chaperones Hsp40 (catalog number SPP-400), Hsp70 (catalog number ESP-555) and Hsp90 (catalog number SPP-776) were provided by Assay Designs (Ann Arbor, MI, USA).

2.2. Site-specific mutagenesis

The WT regulatory domain (WT-hPAH (2–120)) and the mutant G46S regulatory domain (G46S-hPAH (2–120)) were obtained by introducing a stop signal in codon 121 of hPAH, by site-directed

mutagenesis (QuikChange^R II, Stratagene), using the pMAL-WT-hPAH vector [17] and pMAL-G46S-hPAH vector [12] as template, respectively. Primers 5′-GACACAGTGCCCTGGT**AA**CCAAGAACCATTCAAGAGC-3′ (forward) and 5′-GCTCTTGAATGGTTCTTGG**TT**ACCAGGGCACTGTGTC-3′ (reverse) used for mutagenesis were provided by Eurogentec, Seraing, Belgium (the mismatch nucleotides are shown in bold type). The authenticity of the mutagenesis was verified by DNA sequencing as described previously [12].

2.3. Expression and isolation of fusion proteins

Expression of both the WT and the mutated form G46S of hPAH and the R-domain of hPAH (residues 2–120) was performed in *E. coli* as fusion proteins (MBP-(pep)$_{Xa}$-hPAH) [17]. The bacteria were grown at 37 °C and the induction of hPAH by 1 mM isopropyl-thio-β-D-galactoside (IPTG) was performed for 24 h at 28 °C. The fusion proteins were purified by affinity chromatography (amylose resin) and centrifuged in a TL-100 Ultracentrifuge (Beckman, USA) for 20 min at 50,000 g before size-exclusion chromatography (SEC) as described [17]. SEC was performed at 4 °C using a HiLoad Superdex 200 HR column (1.6 cm × 60 cm) prepacked from Amersham Biosciences (GE Healthcare, Uppsala, Sweden). The mobile phase consisted of 20 mM Na-Hepes and 0.2 M NaCl, pH 7.0 and the flow rate was 0.38 ml min^{-1}. The tetrameric/dimeric hPAH fusion proteins and the R-domain of hPAH also as a fusion protein were collected and concentrated by Centriplus 30 filter (Amicon, MA, USA). The concentration of purified fusion proteins was measured by the absorption coefficient A_{280} (1 mg ml^{-1} cm^{-1}) = 1.63 [17] for the full-length enzymes and A_{280} (1 mg ml^{-1} cm^{-1}) = 1.34 for the truncated form hPAH (2–120). A colorimetric method [18] was also used in some cases to measure enzyme concentrations, with bovine serum albumin as the standard.

T427P-hPAH [19] and ΔC24-hPAH [20] were expressed as fusion proteins with MBP in *E. coli* and isolated essentially as the G46S mutant protein, except that before SEC the proteins were cleaved for 4 h at 4 °C by factor Xa protease, using a protease to substrate ratio of 1:200 (by mass) to remove the MBP partner.

2.4. Phosphorylation of hPAH fusion protein

The phosphorylation of the fusion protein (tetrameric form) was performed in a reaction mixture containing 0.1 mM ethylene glycol bis-(α-amino ether)-N,N,N′N′-tetraacetic acid, 0.03 mM EDTA, 1 mM DTT, 10 mM MgAc, 60 µM ATP in 15 mM Na-Hepes, pH 7.0, at 30 °C for 1 h [21]. The enzyme concentrations were 20 µM (hPAH) and 100 nM (catalytic subunit) of PKA. The degree of phosphorylation was measured by the electrophoretic mobility shift [6]. The non-phosphorylated fusion protein control was obtained by incubating the enzyme in the absence of added PKA catalytic subunit, under otherwise identical conditions.

2.5. Cleavage of MBP-hPAH fusion proteins and assay of self-association by light scattering

In order to study the time-course for the cleavage of the tetrameric and dimeric MBP-hPAH fusion proteins and the self-association of the released enzyme, the fusion proteins were incubated in a medium containing 20 mM Na-Hepes, 0.1 M NaCl, pH 7.0 at 25 °C, except when stated otherwise. Before assay the tetrameric or dimeric fusion proteins were subjected to high-speed ultracentrifugation at 210,000 g for 15 min at 4 °C. In the standard assay the concentration of the fusion protein was 0.74 mg ml^{-1} and the concentration of factor Xa was adjusted to give a final ratio (by weight) of 1:150 relative to the fusion protein. Parameters as pH, neutral salt concentration, temperature, protein concentration and the presence of substrates (L-Phe and BH$_4$) varied in different experiments as described in the Results section. Self-association of the factor Xa released enzyme was followed in real-time by light scattering, as measured by the increase in apparent absorbance

at 350 nm ($A'_{350} = \log[I_o/(I_p + f \cdot I_d)]$) using an Agilent 8453 Diode Array Spectrophotometer with a Peltier temperature control unit. The change in light scattering was expressed as $\Delta A'_{350}$ by subtracting the background absorbance in the absence of added factor Xa. $\Delta A'_{350}/\Delta t$ is the rate of formation of higher-order oligomers/polymers obtained from the slope of the linear growth phase of each light scattering curve. For every self-association experiment a parallel time-course cleavage analysis was conducted to rule out any change in the cleavage rate of the fusion protein.

2.6. SDS-PAGE analyses

SDS-PAGE analyses were performed in a 10% (w/v) polyacrylamide gel [22]. The gels were stained by Coomassie Brilliant Blue R-250, scanned using VersaDoc 4000 (Bio-Rad) and quantification of the protein bands was obtained by using the Quantity One 1-D Analysis Software (Bio-Rad Laboratories, Hercules, CA, USA).

2.7. Cleavage of G46S-hPAH fusion protein in the presence of chaperones

In order to study the influence of chaperones on the self-association process following cleavage of the mutant enzyme, tetrameric MBP-G46S-hPAH and chaperone were added (together with the factor Xa protease) at a variable molar ratio as described in Results. The experimental conditions were the same as in the cleavage experiments without chaperone, except in the case of the pharmacological chaperone that was dissolved in DMSO and used at a final concentration of 100 µM and 0.83% DMSO. In this case controls were included with 0.83% DMSO.

2.8. Negative staining electron microscopy

For negative staining EM of unpolymerized and polymerized G46S-hPAH Formvar-coated 200 mesh nickel grids (Electron Microscopy Sciences, Fort Washington, USA) were used. The grids were further coated with carbon, stored dust-free in Petri dishes kept at low humidity, and glow-discharged for 15 s prior to use. Negative staining was carried out by first applying 5 µl of a protein solution on the specimen grid. Following absorption for 60 s, the sample drop was removed by blotting with filter paper and the grid was stained twice with 2% aqueous uranyl acetate. After application, the first drop (10 µl) was blotted off immediately, whereafter a fresh drop of the stain was added to the grid for 15 s. After final blotting and drying, the specimens were observed in a Jeol 1230 Electron Microscope operated at 80 kV.

2.9. Thioflavin-T fluorescence assay

The assay was performed according to a standard protocol [23]. Briefly, the thioflavin-T (ThT, Sigma-Aldrich) measurements were made by taking reaction aliquots and diluting them to 1.3 µM hPAH in 20 mM Na-Hepes, 0.1 M NaCl, pH 7.0 containing 20 µM ThT. Immediately following sample preparation the fluorescence was measured in a Perkin-Elmer LS-50B instrument (Perkin-Elmer, Waltham, MA, USA) at 25 °C (constant temperature cell holder) using an excitation of 440 nm and emission of 482 nm, with slit widths for excitation and emission of 3 and 7 nm, respectively, and by averaging four scans. The reported values were corrected by subtracting the background fluorescence of ThT in the absence of protein oligomers and controls with the protein oligomers in the absence of ThT (light scattering).

2.10. ANS fluorescence assay

Binding of 8-anilino-1-naphthalenesulfonic acid (ANS, Sigma-Aldrich) was performed as described by Aukrust et al. [24]. Briefly, 1.3 µM hPAH was incubated with 60 µM ANS in 20 mM Na-Hepes, 0.1 M NaCl, pH 7.0 at room temperature for 5 min in the dark. The fluorescence emission spectra were recorded between 400 and 600 nm (6 nm slit width) at 25 °C using an excitation wavelength of 385 nm (6 nm slit width) on a Perkin-Elmer LS-50B luminescence spectrometer and by averaging four scans.

2.11. Assay of hPAH activity

The hPAH activity was assayed at 25 °C in a standard reaction mixture containing a 0.4 µM subunit (unless otherwise stated) of tetrameric WT or G46S mutant fusion protein forms of hPAH, 1 mM L-Phe, 0.5 mg ml^{-1} bovine serum albumin, 5 mM dithiothreitol, 0.1 mg ml^{-1} catalase, 100 µM ferrous ammonium sulfate in 100 mM Na-Hepes, pH 7.0 [17]. After preincubation (5 min) with L-Phe the reaction was started by adding 75 µM (unless stated otherwise) BH$_4$ to the reaction mixture. The amount of L-Tyr formed after 1 min was measured by high pressure liquid chromatography and fluorimetric detection [25]. The steady-state kinetic data were analyzed by nonlinear regression analysis using the SigmaPlot® Technical Graphing Software and the modified Hill equation of LiCata and Allewel [26] for cooperative substrate binding as well as substrate inhibition [27]. In some experiments, 1 mM L-Phe was added either at the start of the preincubation period or together with 75 µM BH$_4$ at the initiation of the hydroxylation reaction. In this case a 3 min time-course was then followed in order to study the effect of preincubation with L-Phe on the specific activity.

2.12. Computational analysis

An estimation of the free energy of unfolding of the mutant protein was predicted using the CUPSAT server (http://cupsat.tu-bs.de/) [28] and the free energy of folding was predicted using the Concoord/PBSA server (http://ccpbsa.bioinformatik.uni-saarland.de/ccpbsa/) [29]. In order to evaluate the effect on G46S mutation on the secondary structure of the hPAH protein an algorithm based on helix–coil transition theory, AGADIR, was used to predict helical propensity (http://agadir.crg.es/) [30]. To identify the location of hinges in PAH we subjected the apo-rPAH crystal structure (PDB ID: 2PHM) to further analysis using the HingeMaster software program that predicts the hinge location in a protein by integrating existing hinge predictors (TLSMD, StoneHinge, FlexOracle and HingeSeq) with a family of novel hinge predictors based on grouping residues with correlated normal mode motions (http://molmovdb.org/cgi-bin/submit-flexoracle.cgi) [31].

2.13. Statistical analyses

Data obtained from independent measurements are presented as mean ± SD and Student's t-test was conducted for statistic analysis of quantitative data ($P < 0.01$ was considered significant).

3. Results

3.1. Structural effects of the G46S mutation

The ~50 kDa monomer of WT mammalian PAH assembles *in vivo* and on overexpression in bacteria to form tetramers (TMs) and dimers (DMs). Atomic resolution structures of hPAH and rPAH have revealed that the monomer consists of three structural and functional domains, i.e. a regulatory (R), a catalytic (C) and a tetramerization (T) domain [32–34]. On the basis of the 3D structures of the C–T domains of hPAH and the R–C domains of rPAH a composite full-length model has been assembled for the PAH tetramer [8] (Fig. 1A and B). It is organized as an asymmetric dimer of dimers, and the model has the approximate dimensions of 85 Å × 100 Å × 75 Å. The R-domain has an α–β sandwich ($\beta\alpha\beta\beta\alpha\beta$) motif composed of a four-stranded antiparallel β-sheet flanked on one side by two short α-helices and the other side by the C-domain (Fig. 1C). Using the HingeMaster software program [31] (see
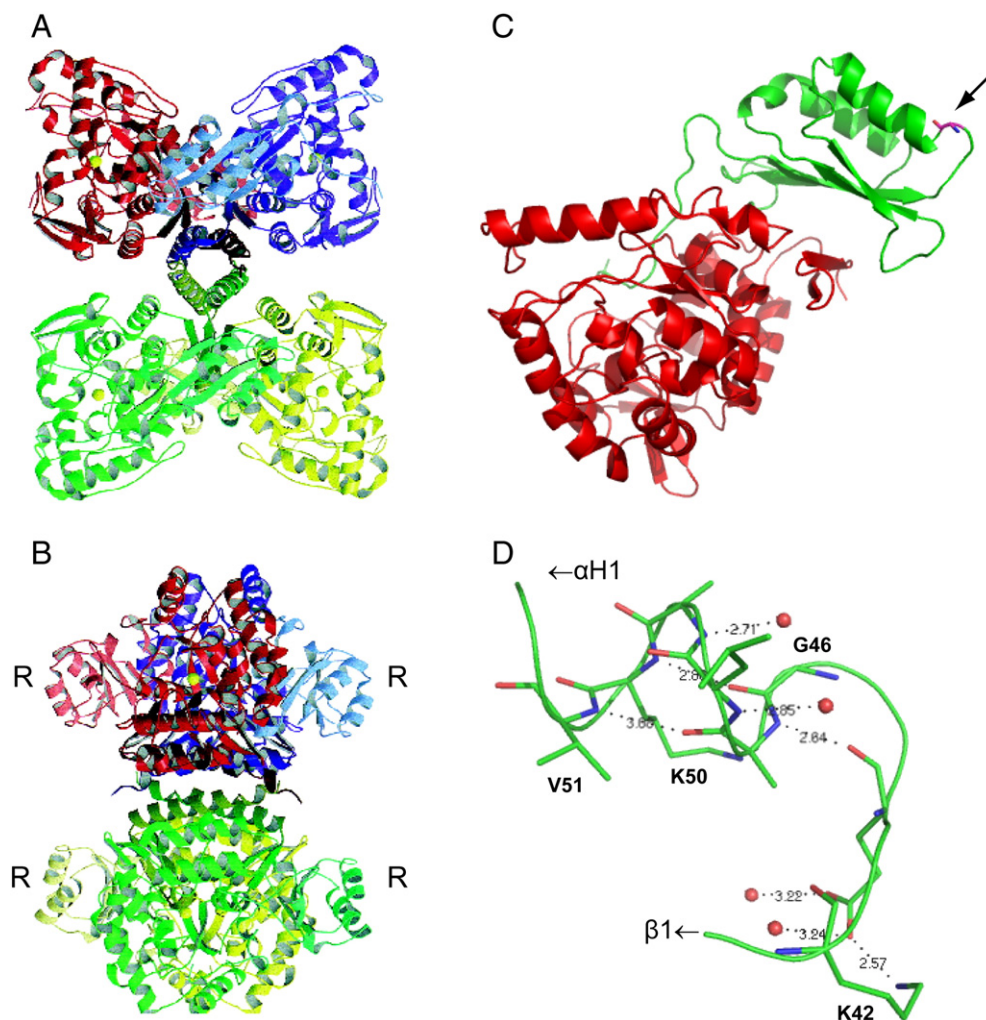
Fig. 1. 3D structure of PAH and the localization/interactions of the G46 residue in the N-terminal regulatory domain. (A) Structure of a composite model of full-length tetrameric hPAH. Cα-trace ribbon of the model created by combining the regulatory/catalytic domain crystal structure of rPAH (PDB ID: 1PHZ) and the catalytic/tetramerization domain structure of hPAH (PDB ID: 2PAH). Each monomer is colored separately, with the lightest color representing the regulatory domain (R) and the darkest color representing the tetramerization domain. (B) Side view 90° rotation from the view in A, with the position of the four regulatory domains indicated by a R. (C) Ribbon representation of the regulatory/catalytic domain crystal structure of rPAH in the monomeric form with the regulatory domain shown in green, the catalytic domain in red and G46 in stick model (pointed arrow). (D) Close-up of the location of G46 in the regulatory domain of rPAH, at the end of the loop between β-strand 1 and α-helix 1, where it H-bonds to K50. The Cα-atom trace is shown in green ribbon, with the relevant residues in stick model and water molecules as red spheres. The figures were created using MOLSCRIPT [76] (A and B) and PyMOL, version 1.1 (DeLano Scientific) [77] (C and D).

Materials and methods) our analysis revealed major hinges in the R–C domain structure around the interdomain residues 118–119 and around the intradomain residues 26–27 (Fig. 2A).

The residue G46 is positioned at the entry of α-helix 1 (A47–E57) in a five residue (L41–G46) loop structure (loop 1), with a relatively low crystallographic *B*-factor (Fig. 2B), linking β-strand 1 and α-helix 1 (Fig. 1D), and is stabilized by H-bonds and a salt-bridge (K42–E44) (Fig. 1D). The α-helix 1 is stabilized at the C-terminal end by forming a hydrophobic interphase with α-helix 2 (not shown). Using the coordinates of the R–C domains (PDB ID: 1PHZ) and two structure-based methods for the estimation of the free energy of unfolding [28] and folding [29] of mutant proteins, substitutions of G46 with any amino acid were found to be destabilizing, and for the G46S mutation the folding free energy was calculated to $\Delta\Delta G = 4.1$ kcal mol^{-1} with a major electrostatic contribution ($\Delta\Delta G_{es} = 4.7$ kcal mol^{-1}). Since Gly is known to have a large destabilizing effect on α-helices [35], whereas a substituted Ser and the preceding residues (V45, E44, E43, K42 and L41) in loop 1 have all a relatively high α-helix-forming propensity [35], the G46 substitution is predicted to promote a N-

terminal extension of α-helix 1 by four residues or one turn using the AGADIR algorithm [30] (Fig. 2C).

3.2. Expression and isolation of the MBP fusion proteins

On expression of WT and the mutant form G46S as fusion proteins (MBP-(pep)$_{Xa}$-hPAH) the proteins were obtained in high yields and separated into their oligomeric forms by SEC (Fig. 3A and B). The chromatogram of both forms revealed a comparable elution pattern in which peak 1 represented higher-order oligomeric forms (eluted at or near the void volume), and peak 3 and peak 4 represented the TM and DM forms, respectively [12,17].

3.3. Catalytic properties of MBP-WT-hPAH and MBP-G46S-hPAH fusion proteins

Determination of the steady-state catalytic properties of the tetrameric MBP-G46S-hPAH fusion protein revealed that it has a higher specific activity than the WT protein, and a slightly higher
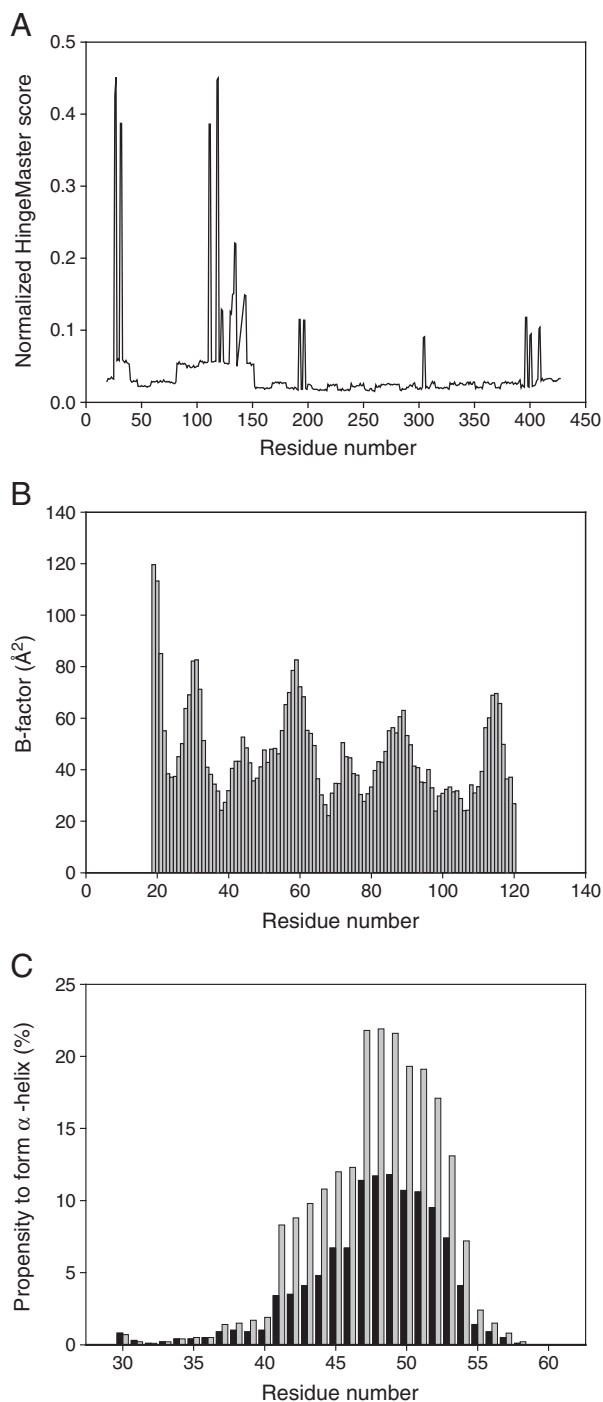
Fig. 2. Structural properties of the regulatory domain. (A) Combined hinge prediction scores of the R–C domain structure in the non-phosphorylated form of rPAH (PDB ID: 2PHM) using the HingeMaster server [31] as a function of amino acid residue number. A similar score profile was obtained for the phosphorylated form (PDB ID: 1PHZ). (B) The crystallographic B-factor values *vs.* residue numbers in the regulatory domain (PDB ID: 1PHZ). (C) Prediction of the effect of the G46 → S substitution on the propensity to form an α-helix in the sequence comprising residues 30 to 58 using the AGADIR algorithm [30]. The black bars represent the propensity to form an α-helix in the WT-PAH protein and the gray bars correspond to the α-helix propensity in the mutant G46S-hPAH.

affinity for the substrate L-Phe ($[S]_{0.5} = 74 \pm 5$ μM for the mutant and $[S]_{0.5} = 106 \pm 2$ μM for MBP-WT-hPAH) (Table 1). The affinity for the cofactor BH$_4$ was unaffected. The mutant fusion protein revealed a low kinetic cooperativity with respect to L-Phe ($n_H = 1.2 \pm 0.1$) and was already in an activated conformational state. Both proteins showed an inhibition at higher substrate concentrations.

3.4. Cleavage of the MBP fusion proteins

In the standard assay conditions the cleavage reaction was similar for the tetrameric WT (not shown) and the mutant fusion protein (Fig. 4A), with $t_{1/2}$ (time at 50% cleavage) of ~11 min. The half-time and the end point of the cleavage reaction varied to some extent with the solvent conditions, notably with the ionic strength (Supplementary Fig. S1A) and the temperature (Supplementary Fig. S1B).

3.5. Self-association of tetrameric and dimeric forms of G46S-hPAH

At the selected standard assay conditions (pH 7.0, 0.1 M NaCl and 25 °C) the cleavage of the MBP-WT-hPAH tetramer (0.74 mg ml^{-1}) did not result in any change in light scattering (Fig. 4B). By contrast, the G46S-hPAH mutant form revealed a propensity to self-associate (Fig. 4B). A sigmoidal time-course was observed for the increase in light scattering with three relatively distinct phases, i.e. a delay period (lag phase), a growth phase of increasing light scattering ($\Delta A'_{350}/\Delta t$ (AU min^{-1}) $= 0.026 \pm 0.003$) and a final phase with a decrease in light scattering. In the absence of added factor Xa no change in light scattering of the MBP-G46S-hPAH fusion protein was observed within the time-scale of 3 h. A comparison of the TM and DM mutant fusion proteins (Fig. 7A) revealed that the DM displayed a similar lag phase but a 2-fold lower $\Delta A'_{350}/\Delta t$ value than the TM (at equal protein concentration) at pH 7.0.

3.6. Effects of pH and ionic strength

WT-hPAH and the R-domain (residues 1–120) have theoretical pIs of ~pH 6.2 and ~pH 6.1, respectively. Whereas no significant difference was observed in the cleavage rate of the fusion protein in the pH interval of 6.4 to 8.0 (Supplementary Fig. S2A), a large effect of pH was observed on the self-association (Fig. 5). Thus, by lowering the pH towards the pI, the lag phase was reduced and the $\Delta A'_{350}/\Delta t$ value greatly increased. At pH 8.0, with a theoretical net charge of ~−9.2 no measurable $\Delta A'_{350}/\Delta t$ value was observed within the time-scale of 3 h.

The ionic strength (range 0.1 M and 0.4 M NaCl) has a certain effect on the rate of cleavage of MBP-G46S-hPAH (Supplementary Fig. S1A), but a more dramatic effect on the lag phase and the $\Delta A'_{350}/\Delta t$ value of G46S-hPAH self-association (Table 2), demonstrating the importance of the global charge in the process.

3.7. Effect of temperature and protein concentration

Whereas the rate of the cleavage was only slightly slower at 15 °C ($t_{1/2}$ of 13.3 min) than at 25 °C ($t_{1/2}$ of 11.3 min) (Supplementary Fig. S1B), the self-association was largely affected by the reaction temperature. Thus, on increasing the temperature the lag phase decreases and the rate of self-association ($\Delta A'_{350}/\Delta t$) increases (Table 2) with an apparent activation energy (E_a) of 134 kJ mol^{-1}.

When the cleavage reaction was followed at the standard assay conditions, but with variable concentrations of fusion protein at a constant ratio of factor Xa:G46S-hPAH = 1:150 (by weight), the half-time was almost the same in the range of 0.37 to 0.74 mg ml^{-1} (Supplementary Fig. S2B). A more pronounced effect was observed on the lag phase and the rate of self-association ($\Delta A'_{350}/\Delta t$) (Table 2).

3.8. The effect of substrates and phosphorylation of Ser16

The binding of L-Phe or the pterin cofactor BH$_4$ at the active site triggers global conformational changes in the WT tetramer, including the R-domain [8]. Here, however, we observed no significant modulation of the self-association of G46S-hPAH in the presence of 75 μM BH$_4$, whereas 1 mM L-Phe slightly reduced the lag phase and increased the $\Delta A'_{350}/\Delta t$ value (Table 2). When the fusion protein was phosphorylated
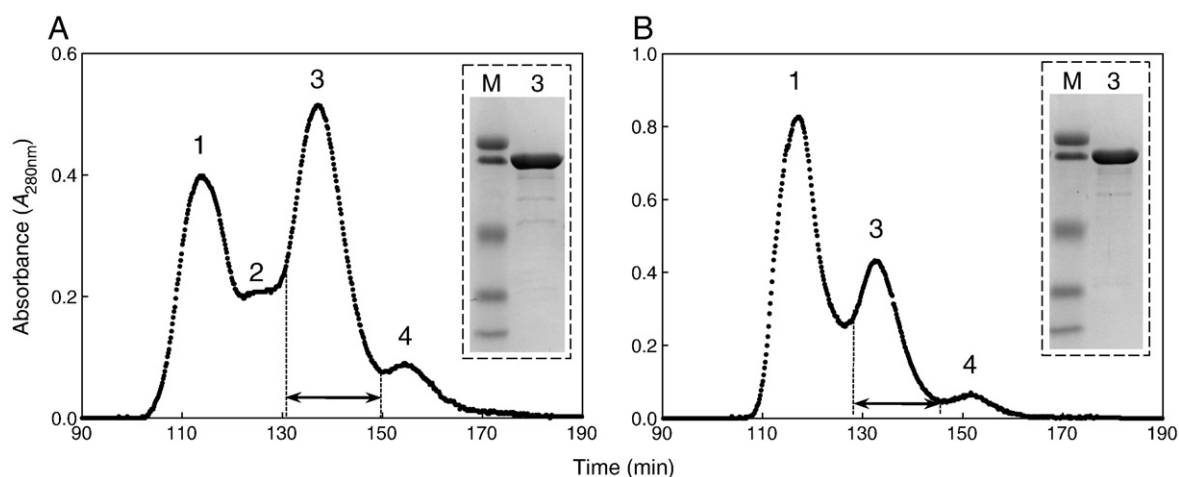
Fig. 3. Size-exclusion chromatography of WT-hPAH and the mutant G46S-hPAH. (A) The chromatogram of WT-hPAH with 4 main peaks, where peak 1 represents higher-order oligomeric forms (eluted in the void volume), peak 2 a presumably octameric form, peak 3 the tetramer (~365 kDa) and peak 4 the dimer (~209 kDa). (B) The chromatogram of the mutant form G46S-hPAH where the broad peak 1 represents higher-order oligomeric forms, peak 3 and 4 the tetramer and dimer, respectively. The apparent molecular mass of the enzyme forms were estimated using the elution position of standard molecular mass markers as a reference (not shown). The two dashed lines indicate the collected tetramers used in further experiments. The proteins were expressed as MBP fusion proteins in *E. coli* under identical expression conditions (24 h, 28 °C). The chromatography was performed on a HiLoad Superdex 200 HR column (1.6 cm×60 cm), equilibrated and eluted with 20 mM Na-Hepes, 0.2 M NaCl, pH 7.0 at a flow rate of 0.38 ml ml^{-1} at 4 °C; detection was at 280 nm. The *inset* in panels A and B represent the SDS-PAGE analyses demonstrating the purity of the tetrameric fusion proteins. *Lane* M, low-molecular-mass standard (106.5, 97.6, 50.2, 36.9 and 28.9 kDa); *lane* 3, the respective tetrameric form enzymes (peak 3) of the size-exclusion chromatography.

at Ser16 to >95%, the self-association of G46S-hPAH was markedly inhibited, with a longer lag phase and a decreased $\Delta A'_{350}/\Delta t$ value (Fig. 6A). The time-courses for the cleavage of the phosphorylated and non-phosphorylated MBP-G46S-hPAH were essentially identical (Supplementary Fig. S2C), and the substrates were without effect on the cleavage of MBP-G46S-hPAH (Supplementary Fig. S2D).

3.9. Effects of heat-shock proteins

Molecular chaperones facilitate the proper folding of many newly synthesized proteins as well as rescue proteins that are misfolded, e.g. due to mutations. Chaperone proteins also exhibit the unique property to inhibit self-association of certain client proteins [36]. From Fig. 6 it is seen that the Hsp70/Hsp40 chaperone system inhibits the self-association of G46S-hPAH in a dose-dependent manner. At the lowest molar ratio (1:20) of Hsp70/Hsp40 there is no effect on the $\Delta A'_{350}/\Delta t$ value, whereas at the higher ratio (1:2) the heat-shock proteins markedly prolong the lag phase and decrease the $\Delta A'_{350}/\Delta t$ value (Fig. 6B). A similar effect was observed for Hsp90 at a molar ratio of 1:2 (Fig. 6C). In control experiments with ovalbumin, no such effects were observed. Moreover, for both chaperones the addition of ATP did not further enhance the modulatory effects observed in the absence of nucleotide (data not shown). The chaperones did not contain cleavage sites for factor Xa restriction protease and were without effect on the cleavage of MBP-G46S-hPAH (Supplementary Fig. S2E).

3.10. Effects of pharmacological and chemical chaperones

The pterin cofactor BH$_4$ has been shown to increase the stability *versus* limited proteolysis by trypsin of WT-hPAH [37], as well as of a number of PKU mutant proteins *in vitro*, and to make them less vulnerable to degradation pathways when expressed in cells [38]. Since the structural basis of the stabilizing effect is quite well understood [37–39] the cofactor is currently used as a pharmacological chaperone in the treatment of a subgroup of PKU/HPA patients [40]. However, as seen from Table 2, BH$_4$ did not have any protective effect on the self-association of G46S-hPAH.

A recent screening of over 1000 pharmacological agents has identified two small-molecule binders (3-amino-2-benzyl-7-nitro-4-(2-quinolyl)-1,2-dihydroisoquinolin-1-one and 5,6-dimethyl-3-(4-methyl-2-pyridinyl)-2-thioxo-2,3-dihydrothieno[2,3-d]pyrimidin-4(1H)-one) as potential therapeutic agents to treat PKU [41]. Here we have found that only 3-amino-2-benzyl-7-nitro-4-(2-quinolyl)-1,2-dihydroisoquinolin-1-one, at a comparable concentration (100 μM), partly inhibits the *in vitro* self-association of G46S-hPAH (Fig. 6D).

The use of osmolytes can produce a chemical chaperoning effect *in vitro* and thus be able to rescue folding defects in proteins involved in conformational disorders [42,43]. In this study we have tested glycerol, trimethylamine N-oxide (TMAO) and (−)-epigallocatechin gallate (EGCG), but only glycerol showed a protective effect, while the other two compounds promoted the self-association (Table 2). The

Table 1
Kinetic properties of tetrameric wild-type hPAH (MBP-WT-hPAH) and G46S-hPAH (MBP-G46S-hPAH) fusion proteins.

	BH$_4$		L-Phe						
	V_{max} (nmol Tyr min^{-1} mg^{-1})	K_m (μM)	V_{max} (nmol Tyr min^{-1} mg^{-1})	$[S]_{0.5}$ (μM)	$k_{cat}/[S]_{0.5}$ (μM^{-1} min^{-1})	n_H	V_i (nmol Tyr min^{-1} mg^{-1})	K_i (μM)	Fold activation R$_{(v+L-Phe/v-L-Phe)}$
MBP-WT-hPAH	3346±151	43±5	2360±33	106±2	2.09	2.5±0.1	1072±218	3190±644	3.9
MBP-G46S-hPAH	4227±187	42±5	3677±104	74±5	4.67	1.2±0.1	1521±131	1911±241	1.1

The catalytic activity was measured as described in the Materials and methods section at 25 °C; the substrate concentrations were 1 mM L-Phe (BH$_4$ variable) and 75 μM BH$_4$ (L-Phe variable). $[S]_{0.5}$ represents the L-Phe concentration at half-maximal activity and $k_{cat}/[S]_{0.5}$ the "catalytic efficiency". The "catalytic efficiency" was calculated on the basis of a subunit molecular mass of 94 kDa.
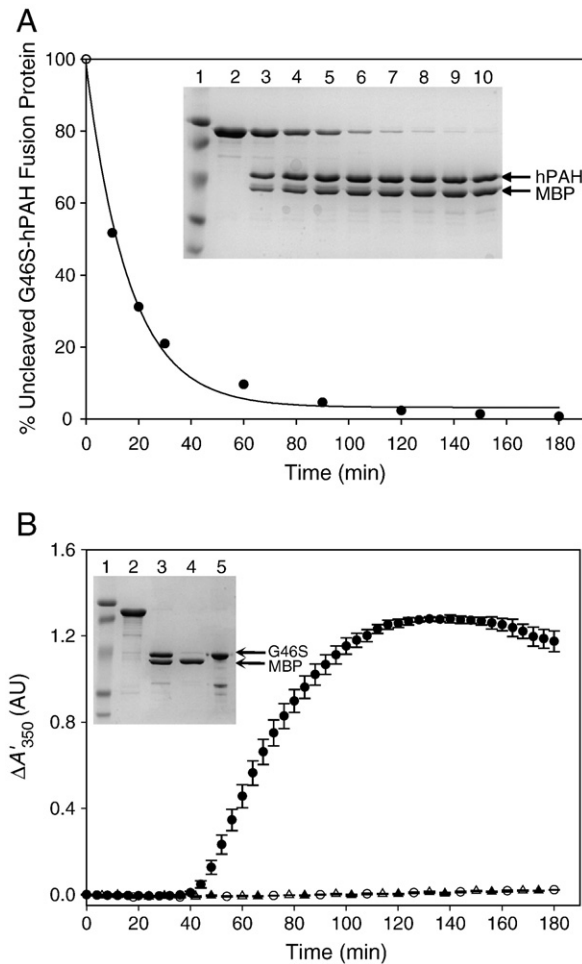
A

B

Fig. 4. The self-association of tetrameric G46S-hPAH following cleavage of the MBP fusion protein by factor Xa. (A) Time-course for the cleavage of tetrameric MBP-G46S-hPAH by the restriction protease factor Xa. The cleavage was performed at standard assay conditions (0.74 mg ml^{-1} fusion protein, 5.0 μg ml^{-1} factor Xa, 20 mM Na-Hepes, 0.1 M NaCl, pH 7.0 and 25 °C). 50% cleavage was obtained at ~11 min ($t_{1/2}$). The data was fitted to a single exponential decay curve. The *inset* represents a 10% SDS-PAGE analysis of the cleavage reaction. Aliquots (4 μg protein) were withdrawn at 0, 10, 20 and 30 min (*lanes 2–5*, respectively), and at 1, 1.30, 2, 2.30 and 3 h (*lanes 6–10*, respectively). *Lane 1*, low-molecular-mass marker (104.4, 83.2, 49.3, 36.9 and 28.9 kDa). (B) Self-association of the released enzyme was followed in real-time by light scattering, as measured by the increase in the apparent absorbance at 350 nm ($A'_{350} = \log [I_o/(I_p + f \cdot I_d)]$) using an Agilent 8453 Diode Array Spectrophotometer. The change in light scattering was expressed as $\Delta A'_{350}$ by subtracting the background absorbance in the absence of the added factor Xa. The data points correspond to G46S-hPAH fusion protein following cleavage by factor Xa (●), and in the absence of factor Xa (○); WT-hPAH fusion protein following cleavage by factor Xa (▲) and in the absence of factor Xa (△). Some data points were omitted for clarity. The reactions were performed at standard assay conditions. Error bars represent mean ± SD, *n* = 3–5 independent experiments. The *inset* represents SDS-PAGE analysis of the G46S-hPAH fusion protein at *t* = 0 (*lane 2*), and following its cleavage by factor Xa at *t* = 180 min (*lane 3*). The reaction mixture (after 180 min) was subjected to ultracentrifugation at 200,000 *g* and both the supernatant (*lane 4*) and pellet (*lane 5*) were recovered and analyzed by 10% SDS-PAGE. *Lane 1*, low-molecular-mass marker (104.4, 83.2, 49.3, 36.9 and 28.9 kDa).

pharmacological and chemical chaperones at the concentrations tested were without effect on the cleavage of MBP-G46S-hPAH (Supplementary Fig. S2D and F).

3.11. Effects of WT-hPAH dimer and ΔC24-hPAH dimer on the self-association of G46S-hPAH dimer

Since the G46S-hPAH tetramer self-associates to higher-order oligomers at a 2-fold higher rate than the dimer (Fig. 7A), it was of interest to see if a molar excess of the WT-hPAH dimer, which does not self-associate beyond the tetramer (data not shown), has any effect on the
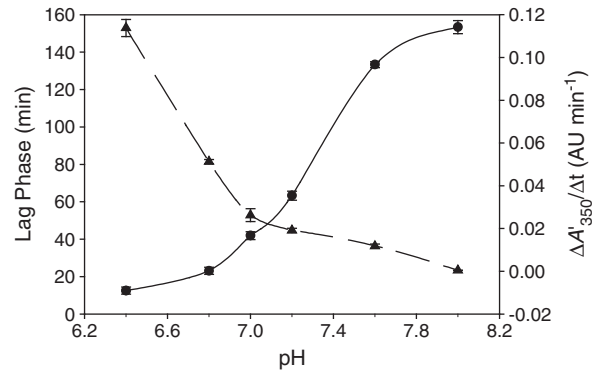

Fig. 5. The effect of pH. The effect of pH on the lag phase (●) and the rate of self-association ($\Delta A'_{350}/\Delta t$) (▲) of G46S-hPAH tetramer at otherwise standard assay conditions. Error bars represent mean ± SD.

self-association of G46S-hPAH dimer. From Fig. 7B it is seen that the WT-hPAH dimer at a 5-fold molar excess markedly shortens the lag phase and increases the $\Delta A'_{350}/\Delta t$ value about 2-fold, presumably by promoting the formation of G46S-WT heterotetramers (see Discussion). By contrast, a 5-fold molar excess of the truncated ΔC24-hPAH dimer, lacking the tetramerization domain, only slightly shortens the lag phase, whereas the rate of self-association ($\Delta A'_{350}/\Delta t$) is almost the same as for the G46S-hPAH dimer alone or in the presence of a 5-fold molar excess of ovalbumin (Fig. 7B). A dimeric mutant form (T427P-hPAH), with a reduced tendency to form tetramer [19], promotes a lower rate of self-association of the G46S-hPAH dimer than the WT-hPAH dimer (Fig. 7B). Moreover, the G46S-hPAH dimer in the presence of a 5-fold molar excess WT-hPAH dimer and 1 mM L-Phe, displayed almost the same lag phase as for the G46S-hPAH dimer alone and only a slightly increased $\Delta A'_{350}/\Delta t$ value (Fig. 7C). In this case the presence of L-Phe promotes the formation of WT tetramer [17]. The presence of 1 mM L-Phe has a negligible effect on the self-association pattern of the G46S-hPAH dimer alone (Fig. 7C) indicating that the G46S dimer ↔ G46S tetramer equilibrium is less responsive to L-Phe than that of WT-hPAH.

Table 2
The effect of solvent conditions, protein concentration, substrates and chemical chaperones on the self-association of tetrameric G46S-hPAH.

		Lag phase (min)	$\Delta A'_{350}/\Delta t$[a] (AU min^{-1})	$(\Delta A'_{350})_{max}$ (AU)
[NaCl]	100	41.9 ± 2.1	0.026 ± 0.003	1.24 ± 0.04
(mM)	200	112.1 ± 3.3	0.007 ± 0.001	0.49 ± 0.09
	400	118.5 ± 2.1	0.000 ± 0.000	0.03 ± 0.01
Temperature	15	87.5 ± 8.0	0.006 ± 0.002	0.49 ± 0.17
(°C)	25	41.9 ± 2.1	0.026 ± 0.003	1.24 ± 0.04
[G46S-hPAH fusion protein]	0.37	79.5[b]	0.014[b]	0.85[b]
(mg ml^{-1})	0.49	44.3[b]	0.017[b]	0.91[b]
	0.74	41.9 ± 2.1	0.026 ± 0.003	1.24 ± 0.04
L-Phe	0	41.9 ± 2.1	0.026 ± 0.003	1.24 ± 0.04
(mM)	1	38.7 ± 4.3	0.035 ± 0.009	1.30 ± 0.14
BH$_4$	0	41.9 ± 2.1	0.026 ± 0.003	1.24 ± 0.04
(μM)	75	45.7 ± 4.0	0.021 ± 0.008	1.22 ± 0.15
Glycerol	0	41.9 ± 2.1	0.026 ± 0.003	1.24 ± 0.04
(%)	1	49.6 ± 3.3	0.020 ± 0.004	1.13 ± 0.16
	2.5	55.9 ± 1.3	0.011 ± 0.001	0.84 ± 0.04
	5	95.3 ± 5.1	0.004 ± 0.001	0.33 ± 0.08
Trimethylamine *N*-oxide	0	41.9 ± 2.1	0.026 ± 0.003	1.24 ± 0.04
(TMAO)	5	39.8[b]	0.032[b]	1.35[b]
(mM)	150	31.8[b]	0.039[b]	1.59[b]
	250	30.5 ± 3.5	0.048 ± 0.008	1.68 ± 0.19
(−)-Epigallocatechin gallate	1:0	41.9 ± 2.1	0.026 ± 0.003	1.24 ± 0.04
(EGCG)	1:0.1	28.6 ± 1.3	0.038 ± 0.001	1.27 ± 0.01
(G46S-hPAH:EGCG)	1:1	23.3 ± 2.4	0.113 ± 0.014	2.37 ± 0.14

[a] $\Delta A'_{350}/\Delta t$ is the rate of formation of higher-order oligomers/polymers as obtained from the slope of the linear growth phase of each light scattering curve. Values are shown as mean ± SD (n = 3–5).
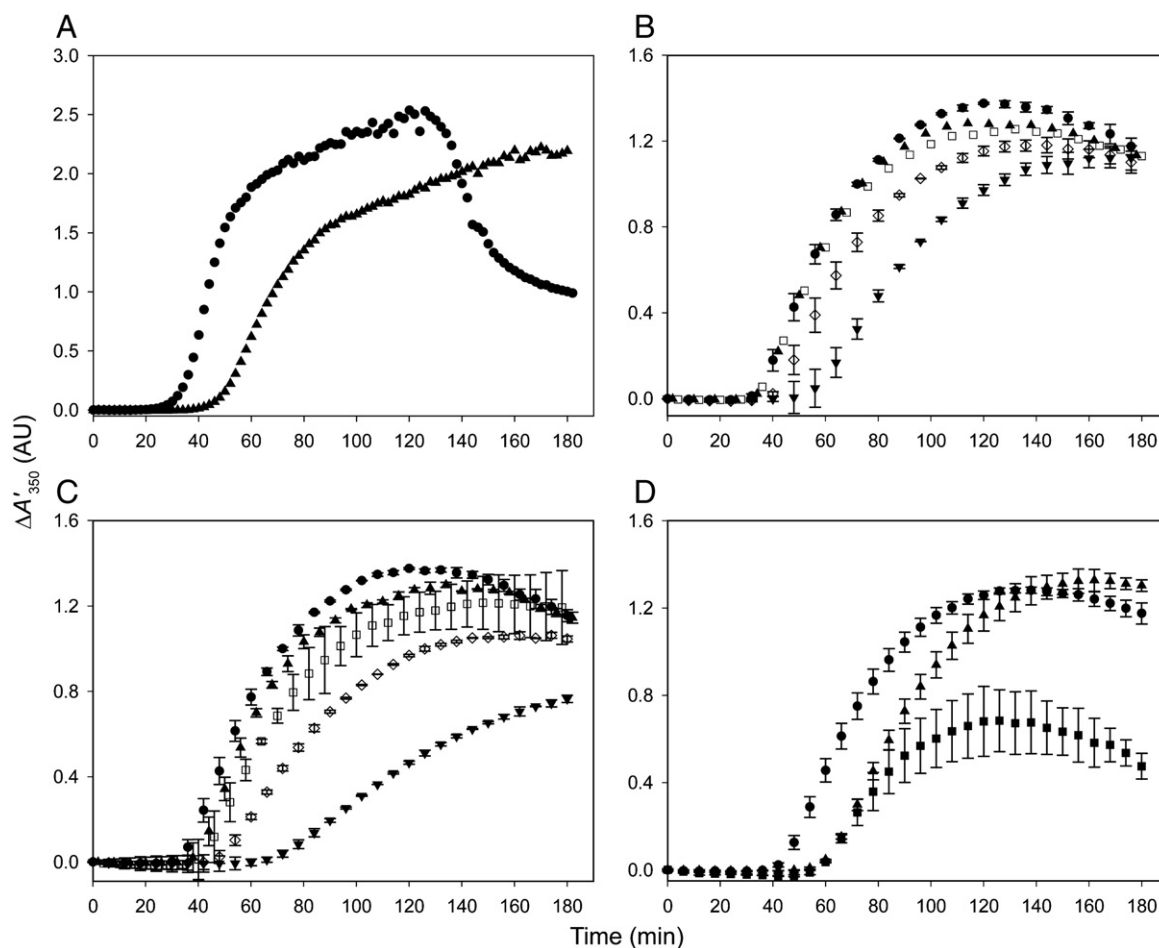[b] SD not determined.

Fig. 6. Effect of phosphorylation at Ser16 and chaperones on the self-association of tetrameric G46S-hPAH. (A) The time-course for the self-association of phosphorylated enzyme (▲) and non-phosphorylated enzyme (●). The non-phosphorylated fusion protein control was obtained by incubating the enzyme in the absence of added PKA catalytic subunit, under otherwise identical conditions of the phosphorylated enzyme. Results are representative of two independent experiments. (B) The effect of Hsp70/Hsp40 (molar ratio 100:1) on the self-association of G46S-hPAH at different concentrations (expressed as molar ratios of chaperone:G46S-hPAH fusion protein): 0:1 (●), 1:20 (▲), 1:10 (□), 1:5 (◇) and 1:2 (▼). (C) The effect of Hsp90 on the self-association of G46S-hPAH at different concentrations (expressed as molar ratios of chaperone:G46S-hPAH fusion protein): 0:1 (●), 1:20 (▲), 1:10 (□),1:5 (◇) and 1:2 (▼). (D) The effect of a pharmacological chaperone on the time-course of the self-association. The data points represent G46S-hPAH in the absence of any added compound (●), in the presence of 0.83% DMSO (▲) or of 100 μM 3-amino-2-benzyl-7-nitro-4-(2-quinolyl)-1,2-dihydroisoquinolin-1-one (in 0.83% DMSO) (■). The self-association reactions were performed at standard assay conditions (0.74 mg ml^{-1} fusion protein (7.85 μM monomer), 5.0 μg ml^{-1} factor Xa, 20 mM Na-Hepes, 0.1 M NaCl, pH 7.0 and 25 °C). Some data points were omitted for clarity. Error bars represent mean ± SD, ($n = 3$).

3.12. Binding of thioflavin-T and ANS

Thioflavin-T (ThT) is a dye that when bound to amyloid fibrils displays an enhanced fluorescence at 482 nm, but nonspecific binding to some non-amyloid proteins has also been reported [23]. Binding of ThT to MBP-WT-hPAH results in a fluorescence enhancement (ΔThT) beyond that of MBP alone, but did not significantly increase ($P = 0.13$) upon cleavage by factor Xa (Fig. 8A). The MBP-G46S-hPAH fusion protein revealed a significantly higher ΔThT-value than MBP-WT-hPAH ($p < 0.01$), and factor Xa cleavage further increased the fluorescence enhancement ($p < 0.01$). About 50% of the total ΔThT-value (at 3 h) was observed during the lag period (~42 min) in which no light scattering (and fibril formation) was observed (Fig. 8B). Moreover, during the period of exponential increase in light scattering the ΔThT represented only 37% of the total fluorescence response. Thus, the ThT fluorescence enhancement of G46S-hPAH vs the WT-hPAH protein is dominated by the cleavage of the fusion protein and a related conformational change.

ANS is a spectroscopic probe that has affinity for hydrophobic clusters which are not tightly packed in a fully folded structure, or become exposed in partially unfolded structures [44]. ANS binds to G46S-hPAH fusion protein (Fig. 8C, *trace* 5) with an increase in the fluorescence intensity and a maximum at ~478 nm (blue shift). Since

this fluorescence response is higher than that observed for the WT-hPAH fusion protein (Fig. 8C, *trace* 3), the mutant form has more hydrophobic clusters exposed than the WT-hPAH. However, after cleavage the fluorescence intensity of the mutant form G46S-hPAH (Fig. 8C, *trace* 7) is only slightly higher than that of the fusion protein (Fig. 8C, *trace* 5). The MBP fusion partner has a negligible contribution to the ANS fluorescence (Fig. 8C, *trace* 2).

3.13. Self-association of the isolated regulatory domain

To further assess the importance of the R-domain for the self-association of full-length G46S-hPAH, we generated WT and G46S truncated forms including the N-terminal residues 2–120 (R-domain) and examined their oligomeric state as MBP fusion proteins and propensity to self-associate on factor Xa cleavage. On bacterial expression as MBP fusion proteins and affinity purification the WT form was recovered in high yield as a mixture of dimer and monomer (Supplementary Fig. S3A), whereas the recovery of the mutant form was very low with higher-order oligomers as the predominating species (Supplementary Fig. S3B). Moreover, SDS-PAGE revealed that the mutant form was significantly more proteolysed than the WT form (Supplementary Fig. S3A and B, *inset*). On cleavage of the dimeric fusion proteins by factor Xa both proteins self-associate with a similar time-
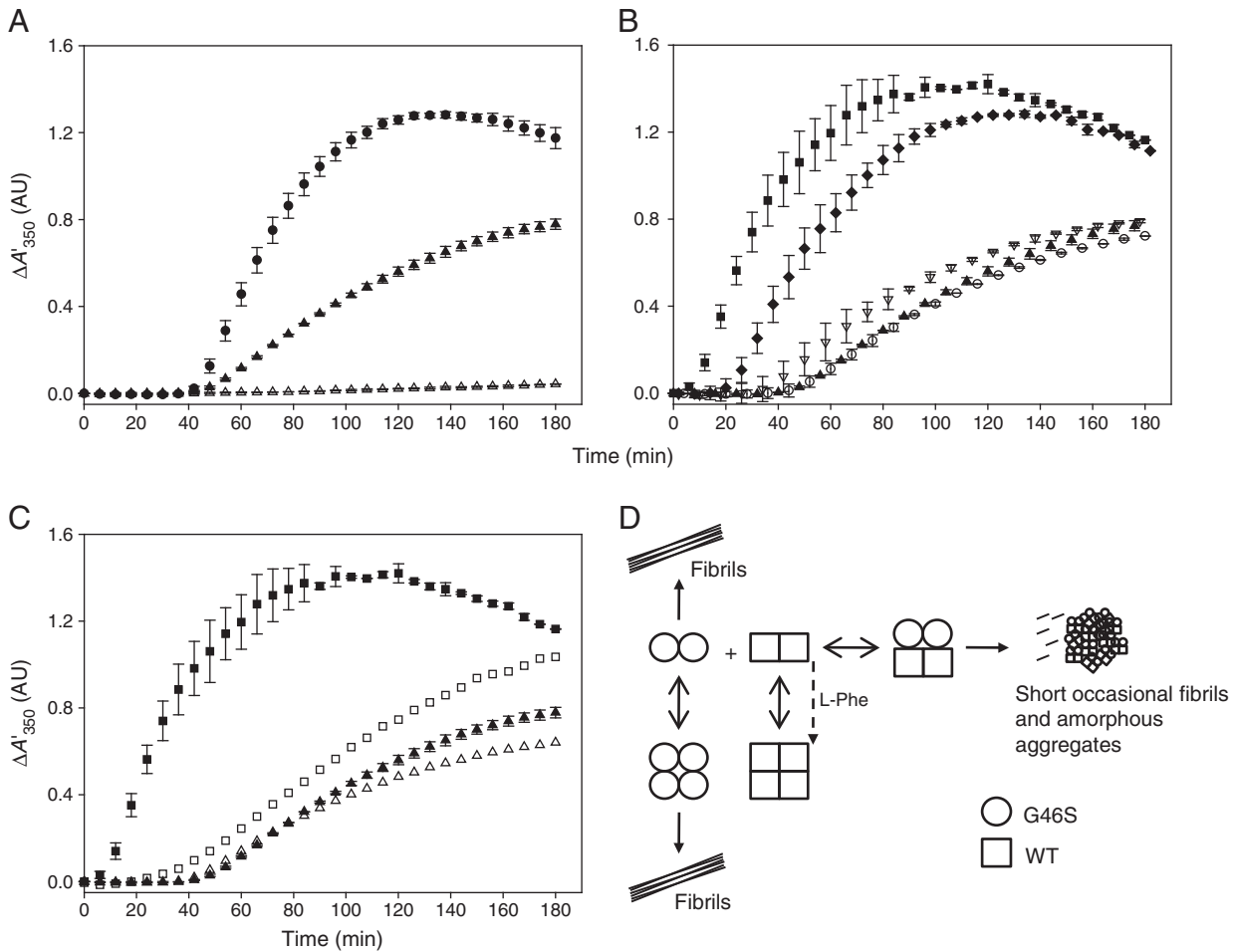
Fig. 7. The self-association of G46S-hPAH dimers and the effect of WT-hPAH dimers and L-Phe. (A) The time-course for the self-association of G46S-hPAH tetramers (●) and dimers (▲) following cleavage of the respective fusion proteins by factor Xa. (△) G46S-hPAH dimer fusion protein in the absence of factor Xa. (B) The self-association of G46S-hPAH dimers in the absence of any added protein (▲), and in the presence of a 5-fold molar excess (5×) of WT-hPAH dimer (■), or of 5×ΔC24-hPAH dimer (▽), or of 5×T427P-hPAH dimer (♦) or of 5×ovalbumin (○). (C) The effect of L-Phe on the self-association of G46S-hPAH dimers in the absence and presence of WT-hPAH dimers. G46S-hPAH dimers in the absence of any added protein and L-Phe (▲) or with 1 mM L-Phe (△); G46S-hPAH dimers in the presence of a 5-fold molar excess of WT-hPAH dimers with no L-Phe (■) or with 1 mM L-Phe (□). (D) Schematic presentation of the G46S-WT homo- and heterotetramer formation. The reactions in (A–C) were performed at standard assay conditions (0.74 mg ml^{-1} fusion protein, 5.0 μg ml^{-1} factor Xa, 20 mM Na-Hepes, 0.1 M NaCl, pH 7.0 and 25 °C) and the WT-hPAH, ΔC24-hPAH and T427P-hPAH enzyme forms were added as already factor Xa cleaved forms. Some data points were omitted for clarity. Error bars represent mean ± SD, ($n = 3$).

course, including a lag period and an exponential phase of increasing light scattering (Fig. 8D). Self-association of the WT protein was inhibited by both substrates (L-Phe > BH$_4$), whereas self-association of the G46S mutant R-domain remained unaffected. In both conditions the L-Phe substrate had no effect on the cleavage by factor Xa (Supplementary Fig. S3C and D). The formation of higher-order oligomers gave only a minor enhancement of the ThT fluorescence (Fig. 8A) and no fibrils were detected on EM (data not shown).

3.14. Ultrastructure of G46S-hPAH polymers

In order to get information on the structure of the higher-order oligomers that are formed after cleavage of the G46S-hPAH fusion protein, negative staining EM was performed. For the WT-hPAH no significant difference was observed in the EM pattern when comparing time points 0 and 180 min (data not shown). By contrast, the G46S-hPAH (Fig. 9A–E) revealed a variety of higher-order structures in a time-dependent fashion. At the end of the delay period small clusters of higher-order oligomeric structures of tetrameric G46S-hPAH were observed (Fig. 9B), followed in time by the appearance of linear polymers (Fig. 9C) (correlating with increased light scattering). These fibrils can bundle together and form branches thereby forming

extensive network structures (Fig. 9D). EM also revealed that some of the long fibrils display an apparent twisted configuration (Fig. 9E). Using high magnification images (*inset* of panel Fig. 9E and Supplementary Fig. S4) the diameters of the fibrils were determined as ~145 Å (the narrowest region) and ~300 Å (the broadest region), using a correction of 15% for the flattening on the electron microscope grid [45]. Interestingly, dimeric G46S-hPAH also generates fibrils with a pronounced tendency to network formation (Fig. 9D), which is inhibited by a 5-fold molar excess of WT-hPAH dimer (Fig. 9F). Additionally, the pharmacological chaperone 3-amino-2-benzyl-7-nitro-4-(2-quinolyl)-1,2-dihydroisoquinolin-1-one inhibits the formation of fibrils by tetrameric G46S-hPAH (Fig. 9G).

4. Discussion

4.1. Self-association of G46S-hPAH in vitro

The isolated tetrameric/dimeric MBP-(pep)$_{Xa}$-G46S-hPAH fusion protein is recovered in a soluble metastable form, stabilized by MBP as a chaperone. When cleaved by the restriction protease factor Xa the released free enzyme is destabilized and forms different types of higher-order oligomers and polymers (fibrils), as determined by
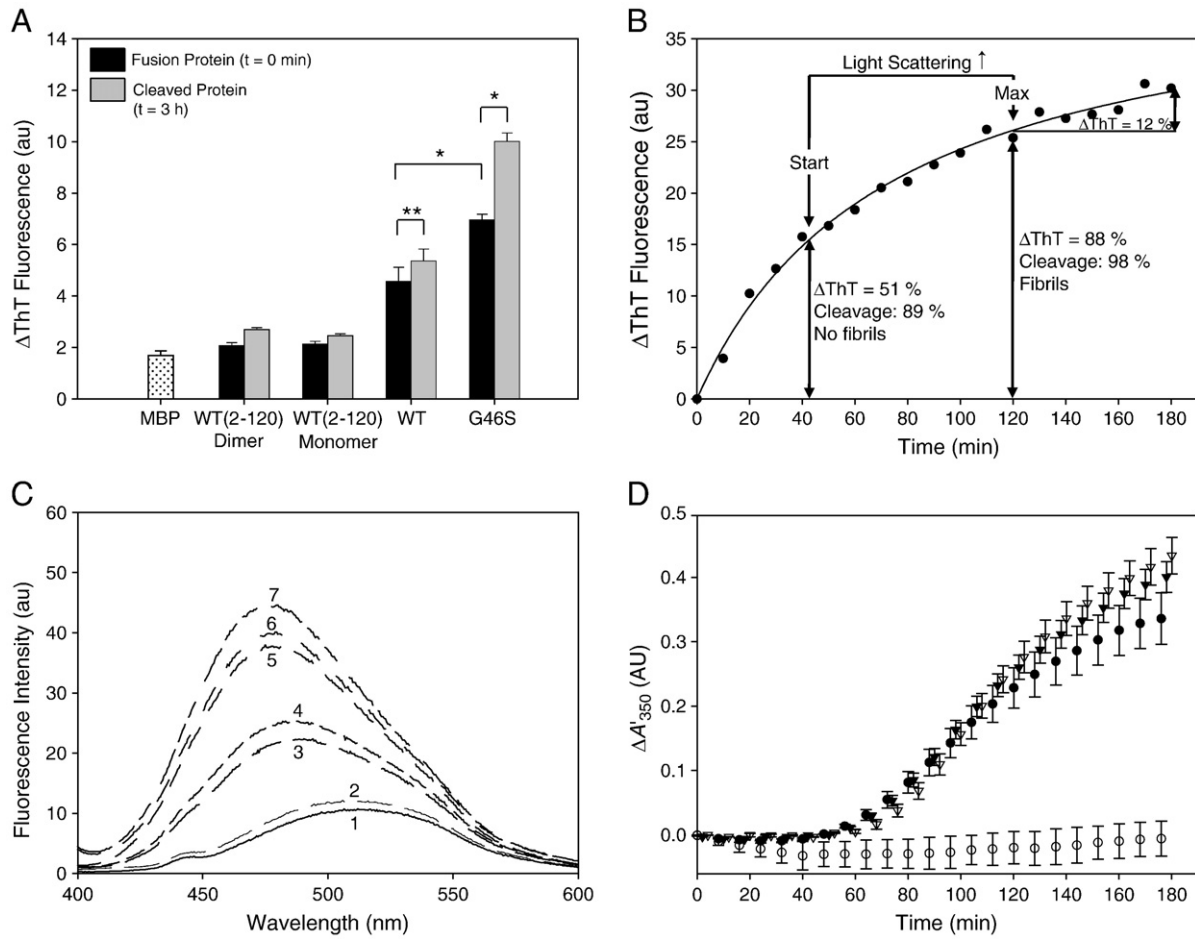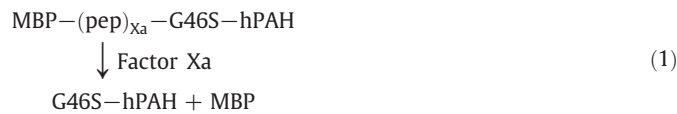
Fig. 8. The binding of thioflavin-T (ThT) and ANS. The binding of ThT and ANS to the uncleaved and cleaved MBP fusion proteins of truncated (residues 2–120, R-domain) and full-length forms of WT and G46S mutant hPAH. (A) ThT fluorescence enhancement (ΔThT) was measured on samples at the beginning of the cleavage reaction of the respective fusion proteins by factor Xa and at the end point ($t = 3$ h). The response was normalized by subtracting the background fluorescence of ThT and light scattering contribution, and the values represent means ± SD of three independent experiments (*$P < 0.01$, **$P = 0.13$). (B) Time-course of the ThT fluorescence enhancement following cleavage of the MBP-G46S-hPAH, including the lag phase (~42 min) and the exponential self-association (78 min), as measured by light scattering and EM (78 min). The start and maximum of light scattering from Fig. 4B is indicated, as well as the change in ThT fluorescence (ΔThT) at selected time points, with the percentage of cleavage specified (Fig. 4A). (C) ANS fluorescence emission spectra observed during the cleavage of MBP-G46S-hPAH fusion protein by factor Xa, i.e. at $t = 0$ min (trace 5), at $t \sim 42$ min (trace 6) and at $t = 3$ h (trace 7). The corresponding spectra for the cleavage of MBP-WT-hPAH fusion protein are shown for comparison at $t = 0$ min (trace 3) and $t = 3$ h (trace 4). The MBP protein was used as a control (trace 2) and the emission spectrum of buffer with ANS is shown (trace 1). The excitation wavelength was 385 nm. (D) The self-association of a truncated form (residues 2–120, R-domain) of WT-hPAH and its G46S mutant form and the effect of the substrate (L-Phe). The time-course of the self-association of WT-hPAH (2–120) dimeric protein following cleavage of the fusion protein by factor Xa in the absence (●) and presence of 150 μM L-Phe (○); G46S-hPAH (2–120) dimer fusion protein following cleavage by factor Xa in the absence (▼) and presence of 150 μM L-Phe (▽). The assays were performed at standard assay conditions and error bars represent mean ± SD, $n = 3$ independent experiments.

light scattering (Fig. 4B) and negative staining EM (Fig. 9B–E). The formation of polymers involves at least three elementary processes: (i) the cleavage of the fusion protein with release of the free enzyme tetramer/dimer,

$$\text{MBP}-(\text{pep})_{\text{Xa}}-\text{G46S}-\text{hPAH}$$
$$\downarrow \text{Factor Xa} \qquad\qquad (1)$$
$$\text{G46S}-\text{hPAH} + \text{MBP}$$

and (ii) self-association with the formation of higher-order oligomers/short polymers [(G46S-hPAH)$_n$], detectable by EM (Fig. 9B) and to some extent by light scattering at 350 nm,

$$n \cdot \text{G46S}-\text{hPAH}$$
$$\downarrow \qquad\qquad (2)$$
$$(\text{G46S}-\text{hPAH})_n$$

and (iii) the autocatalytic formation of larger structures [(G46S-hPAH)$_{m \cdot n}$], detectable by light scattering and EM (Fig. 9C and E),

$$m \cdot (\text{G46S}-\text{hPAH})_n$$
$$\downarrow \qquad\qquad (3)$$
$$(\text{G46S}-\text{hPAH})_{m \cdot n}$$

On cleavage, the light-scattering versus time profile (Fig. 4B) can be divided into a delay period (lag phase) and a growth phase with an autocatalytic formation of higher-order oligomers/polymers that is expressed as $\Delta A'_{350}/\Delta t$ in the relatively linear part of the light scattering increase. At the end point a decrease in light scattering was observed at acidic pH, low ionic strength and temperature >15 °C, caused by the sedimentation of protein at 1 g. By comparing the time-course for the cleavage (Fig. 4A) with the delay time (Fig. 4B), it can be concluded that the cleavage is not rate-limiting in the overall reaction leading to the formation of hPAH polymers, most clearly seen at a low temperature (Supplementary Fig. S1B and Table 2). The delay time

and the rate $\Delta A'_{350}/\Delta t$ were both found to be very sensitive to pH, neutral salt ionic strength and temperature (Fig. 5 and Table 2). Moreover, the experimental conditions which favor a short delay time also promote a high rate of the autocatalytic process.

4.2. The effects of chaperones

Since the first report on PKU patients responding to oral administration of BH₄ by lowering their blood Phe levels [46], the cofactor has been successfully used for the long-term treatment of HPA patients as an alternative to dietary treatment [47,48]. Based on the BIOPKUdb database (www.bh4.org/BH4DatabasesBiopku.asp) [48] BH₄-responsiveness is expected in about 50% of all patients with PAH deficiency [48]. Interestingly, the responsive mutations are preferentially located to the R-domain, possibly related to its structural and physico-chemical properties (see below), and the effect on its stability by the specific interaction with the 1′,2′-dihydroxypropyl side-chain of BH₄, when bound at the active site of WT-hPAH [16,37]. A positive clinical response to BH₄ has been reported even in a patient with severe PKU and the genotype G46S/S303A [47], but it was concluded that the S303A allele was responsible for the observed decrease in plasma Phe level caused by oral BH₄. The present *in vitro* study (Table 2) further supports the conclusion that the G46S allele is non-responsive to BH₄.

Due to the mutant selectivity and the high cost of BH₄ alternative pharmacological chaperones have been explored. A recent screening of over 1000 pharmacological agents has identified a small-molecule binder (3-amino-2-benzyl-7-nitro-4-(2-quinolyl)-1,2-dihydroisoqui-nolin-1-one) that efficiently enhances the thermal stability of WT-PAH and misfolded mutant forms in the R-domain (I65T and R68S), and significantly increases the activity and steady-state PAH protein levels in transiently transfected cells [41]. Here we have found that this small-molecule binder, used at a comparable concentration (100 μM), partly inhibits the self-association of G46S-hPAH, as measured by light scattering (Fig. 6D) and completely inhibits the fibril formation (Fig. 9G).

Glycerol and trimethylamine N-oxide (TMAO) have been shown to correct folding/assembly defects of some neurodegenerative and metabolic conformational disorders [49–53]. In this study glycerol had a protective effect, with a delayed lag phase and decreased $\Delta A'_{350}/\Delta t$ value, whereas TMAO promoted the self-association (Table 2). A similar promotive effect was observed for (−)-epigallocatechin gallate (EGCG) (Table 2), the major polyphenol in green tea that was recently shown to inhibit the fibrillogenesis of amyloidogenic polypeptides [54].

4.3. The self-association of G46S-hPAH generates non-amyloid fibrils

With reference to the ThT fluorescence response (Fig. 8A and B) and the ultrastructures observed by EM (Fig. 9), three lines of evidence point to the formation of non-amyloid fibrils. First, in the self-association of G46S-hPAH the initial part (~51%) of the hyperbolic time-course for ThT fluorescence enhancement occurs in the lag phase (~42 min) where no increase in light scattering or formation of fibrils was observed. In the self-association of proteins forming amyloid-like fibrils the ThT fluorescence enhancement is related to the fibril formation [55]. Thus, the initial fluorescence enhancement of G46S-hPAH is related to the main cleavage of the fusion protein (~89%), presumably reflecting a conformational change in its R-domain, since no fluorescence enhancement was observed on cleavage of the WT-hPAH fusion protein (Fig. 8A). Such unspecific binding of ThT has been observed for some

other proteins [23,55]. In addition, studies on amyloid-like peptides revealed a poor correlation between ThT fluorescence enhancement and the formation of amyloid-like structures [56]. Secondly, the ΔThT value increased by only 37% during the autocatalytic formation of fibrils (Fig. 8B), partly explained by the residual cleavage of the fusion protein. Thirdly, the fibrils generated by G46S-hPAH are highly branched (Fig. 9 and Supplementary Fig. S4A) forming networks, and the diameters of individual fibrils range from ~145 to 300 Å, whereas amyloid and amyloid-like fibrils appear by EM as rigid, nonbranching structures from ~60 to 130 Å in diameter [57].

The self-association of G46S-hPAH demonstrates some apparent similarities with that of sickle cell hemoglobin (deoxy-HbS). Deoxy-HbS and G46S-hPAH are both misfolded tetrameric proteins, and their self-association is caused by mutations affecting a single surface exposed amino acid (E6V in the β-chain of HbS and G46S in the R-domain of hPAH). The two mutant proteins also display similar kinetic patterns of the self-association process, as measured by light scattering, and they polymerize into a number of ultrastructures as a function of time, initiated by factor Xa cleavage of MBP-G46S-hPAH and by deoxygenation of HbS, respectively [58]. The G46S-hPAH fibrils and those derived from deoxy-HbS also share common properties. At the present resolution (160,000×) the typical fibrillar structures formed by tetrameric G46S-hPAH (Fig. 9E, *inset* and Supplementary Fig. S4A) show the above described periodic variation in apparent diameter, i.e. from ~145 Å (the narrowest region) to ~300 Å (the broadest region). Some of the structures have the appearance of twisted fibrils (Fig. 9C and Supplementary Fig. S4A). By comparison, the corresponding dimensions of the deoxy-HbS fibrils were reported to be 180 and 230 Å [45,59]. However, the self-association of the two proteins involves different molecular mechanisms.

4.4. Structural insight into the self-association of G46S-hPAH

In WT-PAH the R-domain has some unique structural and physico-chemical properties, which may explain why mutations in this domain affect the stability of the enzyme. First, the 3D structure [34] has demonstrated an overall high crystallographic B-factor of the R-domain (Fig. 2B). In the full-length enzyme the R-domain is also characterized by a particularly low thermal stability, as compared to the C-domain [60,61]. The R-domain is partly stabilized by its interaction with the 1′,2′-dihydroxypropyl side-chain of the pterin cofactor BH₄ when bound at the active site [16,37]. Secondly, by using the TANGO algorithm for sequence-dependent prediction of the propensity to aggregate [62], the β1-strand (residues I35–L41) and the β2-strand (residues E76–T81) were predicted to promote aggregation, whereas the G46S substitution did not change this prediction. However, since the WT-hPAH tetramer/dimer, in contrast to the G46S-hPAH tetramer/dimer, does not self-associate at standard experimental conditions (Fig. 4B), the predicted aggregation propensity cannot explain the difference. Of more importance is the prediction (Fig. 2C) that the G46S mutation results in an extension of α-helix 1 by four residues. Such a change of the C_α backbone conformation and the α–β sandwich structure of the WT enzyme may promote new intermolecular contacts and self-association via the mutually misfolded regions of their R-domains (Supplementary Fig. S4B). Thirdly, the inhibitory effect of phosphorylation of Ser16 (Fig. 6A) also indicates that the C_α backbone conformation of the R-domain is important for the self-association process. Moreover, MD simulations of WT-hPAH have revealed that this phosphorylation

Fig. 9. Electron micrographs of negatively stained G46S-hPAH before and after cleavage of its MBP fusion protein by factor Xa. (A) The tetrameric MBP-G46S-hPAH fusion protein before cleavage, and (B) after cleavage for 42 min (~ the end of lag phase, as shown in Fig. 4B), and (C) for 2 h (~ maximum light scattering, Fig. 4B). (D and F) The result of cleavage of the dimeric MBP-G46S-hPAH in the absence (D) and presence of a 5-fold molar excess of dimeric WT-hPAH (F). (E) The twisted fibrils and a single fibril of tetrameric G46S-hPAH (*inset*) at high resolution. (G) The effect of the pharmacological chaperone 3-amino-2-benzyl-7-nitro-4-(2-quinolyl)-1,2-dihydroisoquinolin-1-one on the self-association of tetrameric G46S-hPAH at $t = 3$ h of cleavage. The proteins were negatively stained with aqueous uranyl acetate and analyzed in Jeol 1230 Electron Microscope operated at 80 kV. Short fibrils in B and F are indicated by arrows. Scale bars: 500 nm (A–C, F and G), 1 μm (D) and 100 nm (E).
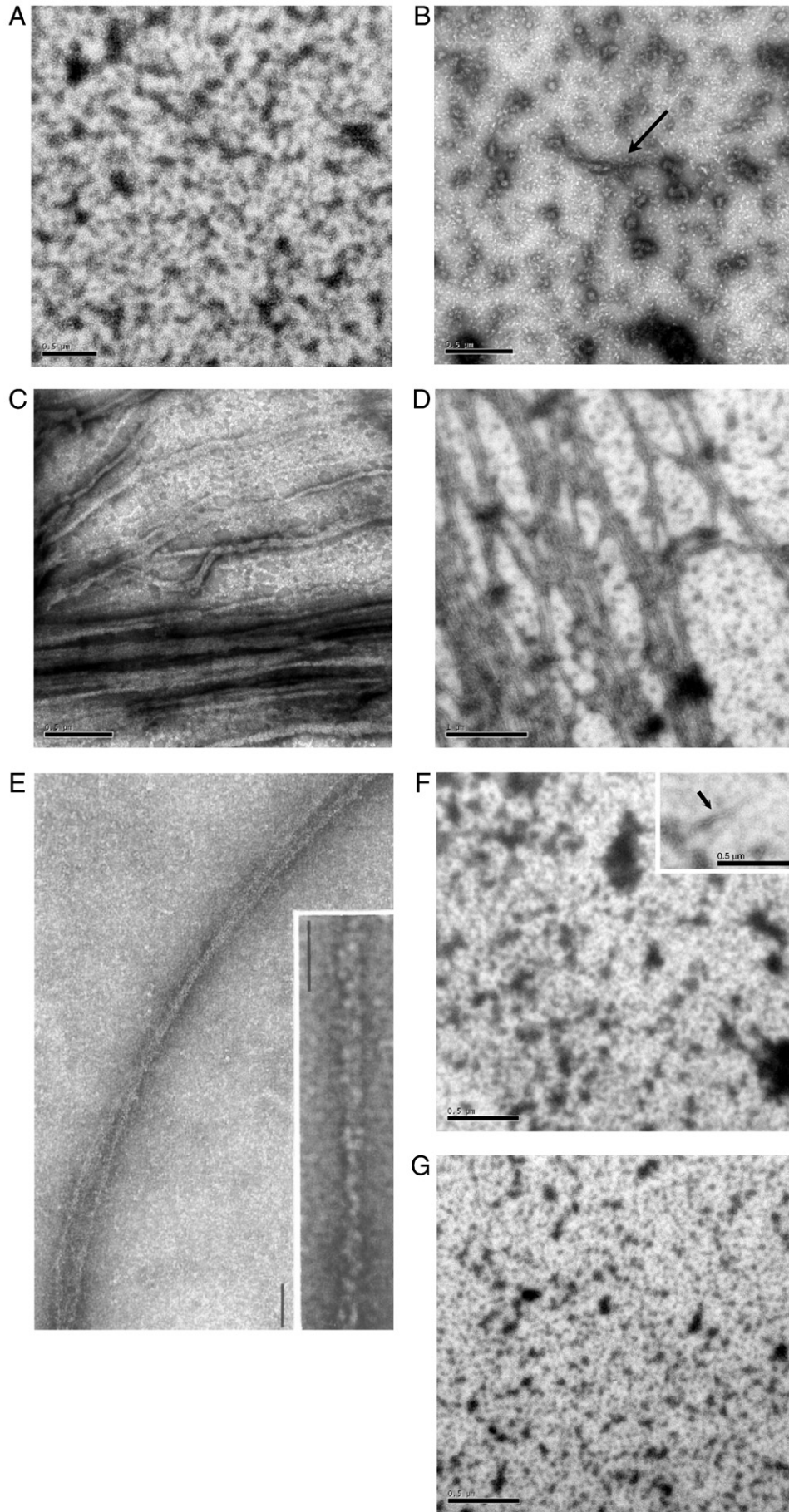
causes local conformational changes in the autoregulatory sequence (residues 1–33) [16], and FT-IR spectroscopy of the isolated WT R-domain (residues 2–110) has suggested that it induces an apparent increase in the α-helix content [15]. In addition, deamidation of labile asparagine residues in hPAH — notably Asn32 in the R-domain [63] — also affects the G46S-hPAH self-association. Accordingly, the non-deamidated form of G46S-hPAH (2 h induction) showed a higher tendency to self-associate (with a slightly shorter lag phase and a higher rate of self-association), as compared with the deamidated G46S-hPAH form (24 h induction) (Supplementary Fig. S5). Studies on the isolated R-domain (residues 2–120) (Fig. 8D) further emphasize the importance of its conformation in the self-association process. The dimeric and monomeric forms of this truncated protein display a high propensity to self-associate, even in their WT forms, and the G46S mutation slightly increased this propensity.

The finding that the G46S-hPAH dimer also self-associates beyond the tetrameric state, although at a slower rate than the tetramer (Fig. 7A), requires a special comment. Since the WT-PAH exists in a two-state TM ↔ DM equilibrium [8], it is likely that a similar equilibrium exists for the G46S-hPAH mutant. As seen from Fig. 7B, the presence of a superstoichiometric amount of WT dimer during the cleavage of the MBP-G46S-hPAH dimer supports the formation of hybrid WT–G46S heterotetramer, which self-associates at an enhanced rate compared to G46S-hPAH dimer alone. In this case, however, EM studies demonstrated predominantly amorphous aggregates (Figs. 7D and 9F). Based on these results one might expect that in a heterozygous WT/G46S genotype, the fraction of the G46S-hPAH dimer could form WT–G46S heterotetramers that would promote the self-association and the degradation of the WT subunit. However, in WT-hPAH the TM ↔ DM equilibrium is shifted towards the tetrameric form in the presence of L-Phe [17], whereas in G46S-hPAH the TM ↔ DM equilibrium is less responsive to L-Phe, as there is only a minor enhancement of the self-association of the G46S-hPAH dimer in the presence of 1 mM L-Phe (Fig. 7C). Because the two equilibria respond differently to L-Phe, the WT-hPAH dimer will form WT-hPAH tetramers in the presence of L-Phe and will not be available to form WT–G46S heterotetramers that were responsible for the observed enhancement of the self-association of the G46S-hPAH dimer in the presence of the WT-hPAH dimer. The concentration of L-Phe (50–100 μM in the hepatocyte of normal individuals), depends on the metabolic state and extracellular concentration of L-Phe in the blood [64]. In a homozygous G46S phenotype the L-Phe will not have any significant effect on the TM ↔ DM equilibrium (Fig. 7C). Thus, our results suggest that the self-association of G46S-hPAH is favored by the tetrameric structure, and the propensity of the G46S-WT hybrids to self-associate is defined by the conformational state of the G46S subunits.

The relation between self-association of a protein, its fundamental physico-chemical intrinsic properties (e.g. hydrophobicity, secondary structure propensity, charge and hydrophobic/ hydrophilic patterns), and extrinsic factors have been extensively studied [65–67]. All the data presented in this study (pH, ionic strength, phosphorylation state of Ser16) indicate that the net charge of the protein, or its R-domain, is a main modulator of the self-association of G46S-hPAH *in vitro*, as measured by light scattering (Table 2).

4.5. Potential in vivo implications

In our previous transfection studies in HEK293 cells the expression level of G46S-hPAH was only ~3% of WT-hPAH (immunoreactive PAH protein) when related to the mRNA levels, compatible with the severe form of PKU observed in the homozygous patient [12]. The present *in vitro* studies offer an explanation for the accelerated degradation of the mutant protein, although we do not know how G46S self-associates in the complex and crowded macromolecular environment of the hepatocyte. Since there is no reported link between any liver dysfunction or amyloid pathology and severe forms of PKU, it is unlikely

that self-associated, misfolded hPAH mutant proteins exert a toxic effect on the liver. Based on inhibition of the self-association of tetrameric G46S-hPAH *in vitro* by substoichiometric concentrations of the heat-shock protein Hsp90 (Fig. 6C), and to some extent by Hsp70/Hsp40 (Fig. 6B), the mutant is a likely client protein of the molecular chaperone systems *in vivo*, as observed for the chaperonins GroESL on co-expression with several PKU/HPA mutant proteins in *E. coli* [5,68,69]. However, the accelerated degradation of G46S-hPAH in HEK293 cells [12] indicates that the physiological level of chaperones in these cells (and in hepatocytes) is not sufficient to rescue this misfolded protein. Therefore, the main question to be answered relates to the mechanism by which G46S-hPAH and related misfolded and unstable hPAH proteins are degraded *in vivo*. Although WT-hPAH is poly/multi-ubiquitinated *in vitro* [70], no significant stabilizing effect of proteasome inhibitors have been observed in cases of selected missense mutations [4]. Therefore, the accelerated turnover observed upon their expression in eukaryotic cells may be explained by an alternative quality control mechanism. Previous studies on the turnover of WT-hPAH in cultured hepatoma cells gave an estimated half-life of 8.2 h [71], i.e. similar to that of a number of other cytosolic liver proteins with a slow turnover, which are considered to be degraded by autophagosome pathway [72]. Intracellular self-association of a number of misfolded proteins has been connected with the formation of aggresomes, which are ultimately degraded by autophagolysosomes, in a process that also involves ubiquitination [73].

4.6. Relevance for the study of misfolding PKU/HPA mutations

The tetrameric form of recombinant WT-hPAH has a small margin of stability. Even a low concentration of a mild denaturant (urea) allows the enzyme to explore a range of different structural states and induces its self-association [74]. Therefore, it is not unexpected to find a high frequency of misfolding hPAH mutations associated with PKU/HPA, resulting in a variety of molecular subtypes showing different conformational and stability properties. Thus, these misfolded hPAH proteins represent a phenotypically heterogeneous group which often has a propensity to self-associate and to form higher-order oligomers when overexpressed in prokaryotic systems, and are rapidly degraded when expressed in eukaryotic cells. Upon overexpression in *E. coli*, these misfolded mutant proteins are often stabilized by MBP as a fusion partner, and the metastable fusion proteins are frequently used in *in vitro* studies to elucidate the molecular basis of the functional impairment in PAH deficiency [9,68,69]. However, the present study shows that the physico-chemical properties of the metastable MBP-mutant-hPAH fusion protein are not representative for those of the mutant protein. Our current experimental approach, therefore, should be a useful supplement in systematic *in vitro* studies of misfolded PAH/HPA-associated mutant proteins, as well as for the assessment of the capability of molecular and pharmacological chaperones to prevent their self-association and stabilize their native states. This experimental approach may also provide valuable mechanistic insights into the frequently observed and poorly understood compound heterozygous forms of PKU/HPA [75].

Appendix A. Supplementary data

Supplementary data to this article can be found online at doi:10.1016/j.bbadis.2010.09.015.

References

[1] L. Hoang, S. Byck, L. Prevost, C.R. Scriver, PAH Mutation Analysis Consortium Database: a database for disease-producing and other allelic variation at the human PAH locus, Nucleic Acids Res. 24 (1996) 127–131.

[2] C.R. Scriver, P.J. Waters, Monogenic traits are not simple: lessons from phenylketonuria, Trends Genet. 15 (1999) 267–272.

[3] T. Flatmark, P.M. Knappskog, E. Bjørgo, A. Martínez, Molecular characterization of disease related mutant forms of human phenylalanine hydroxylase and tyrosine hydroxylase, in: W. Pfleiderer, H. Rokos (Eds.), Chemistry and Biology of Pteridines and Folates, vol. 8, Blackwell Science, Berlin, 1997, pp. 503–508.

[4] P.J. Waters, How PAH gene mutations cause hyper-phenylalaninemia and why mechanism matters: insights from in vitro expression, Hum. Mutat. 21 (2003) 357–369.

[5] N. Gregersen, P. Bross, B.S. Andresen, C.B. Pedersen, T.J. Corydon, L. Bolund, The role of chaperone-assisted folding and quality control in inborn errors of metabolism: protein folding disorders, J. Inherit. Metab. Dis. 24 (2001) 189–212.

[6] E. Bjørgo, P.M. Knappskog, A. Martinez, R.C. Stevens, T. Flatmark, Partial characterization and three-dimensional-structural localization of eight mutations in exon 7 of the human phenylalanine hydroxylase gene associated with phenylketonuria, Eur. J. Biochem. 257 (1998) 1–10.

[7] H. Erlandsen, R.C. Stevens, The structural basis of phenylketonuria, Mol. Genet. Metab. 68 (1999) 103–125.

[8] T. Flatmark, R.C. Stevens, Structural insight into the aromatic amino acid hydroxylases and their disease-related mutant forms, Chem. Rev. 99 (1999) 2137–2160.

[9] S.W. Gersting, K.F. Kemter, M. Staudigl, D.D. Messing, M.K. Danecka, F.B. Lagler, C.P. Sommerhoff, A.A. Roscher, A.C. Muntau, Loss of function in phenylketonuria is caused by impaired molecular motions and conformational instability, Am. J. Hum. Genet. 83 (2008) 5–17.

[10] J.D. Fox, R.B. Kapust, D.S. Waugh, Single amino acid substitutions on the surface of *Escherichia coli* maltose-binding protein can have a profound impact on the solubility of fusion proteins, Protein Sci. 10 (2001) 622–630.

[11] R.B. Kapust, D.S. Waugh, *Escherichia coli* maltose-binding protein is uncommonly effective at promoting the solubility of polypeptides to which it is fused, Protein Sci. 8 (1999) 1668–1674.

[12] H.G. Eiken, P.M. Knappskog, J. Apold, T. Flatmark, PKU mutation G46S is associated with increased aggregation and degradation of the phenylalanine hydroxylase enzyme, Hum. Mutat. 7 (1996) 228–238.

[13] A.L. Pey, F. Stricher, L. Serrano, A. Martinez, Predicted effects of missense mutations on native-state stability account for phenotypic outcome in phenylketonuria, a paradigm of misfolding diseases, Am. J. Hum. Genet. 81 (2007) 1006–1024.

[14] F.F. Miranda, K. Teigen, M. Thorolfsson, R.M. Svebak, P.M. Knappskog, T. Flatmark, A. Martinez, Phosphorylation and mutations of Ser(16) in human phenylalanine hydroxylase. Kinetic and structural effects, J. Biol. Chem. 277 (2002) 40937–40943.

[15] R. Chehin, M. Thorolfsson, P.M. Knappskog, A. Martinez, T. Flatmark, J.L. Arrondo, A. Muga, Domain structure and stability of human phenylalanine hydroxylase inferred from infrared spectroscopy, FEBS Lett. 422 (1998) 225–230.

[16] K. Teigen, A. Martinez, Probing cofactor specificity in phenylalanine hydroxylase by molecular dynamics simulations, J. Biomol. Struct. Dyn. 20 (2003) 733–740.

[17] A. Martinez, P.M. Knappskog, S. Olafsdottir, A.P. Døskeland, H.G. Eiken, R.M. Svebak, M. Bozzini, J. Apold, T. Flatmark, Expression of recombinant human phenylalanine hydroxylase as fusion protein in *Escherichia coli* circumvents proteolytic degradation by host cell proteases. Isolation and characterization of the wild-type enzyme, Biochem. J. 306 (1995) 589–597.

[18] M.M. Bradford, A rapid and sensitive method for the quantitation of microgram quantities of protein utilizing the principle of protein–dye binding, Anal. Biochem. 72 (1976) 248–254.

[19] E. Bjørgo, R.M. de Carvalho, T. Flatmark, A comparison of kinetic and regulatory properties of the tetrameric and dimeric forms of wild-type and Thr427–>Pro mutant human phenylalanine hydroxylase: contribution of the flexible hinge region Asp425-Gln429 to the tetramerization and cooperative substrate binding, Eur. J. Biochem. 268 (2001) 997–1005.

[20] P.M. Knappskog, T. Flatmark, J.M. Aarden, J. Haavik, A. Martinez, Structure/function relationships in human phenylalanine hydroxylase. Effect of terminal deletions on the oligomerization, activation and cooperativity of substrate binding to the enzyme, Eur. J. Biochem. 242 (1996) 813–821.

[21] A.P. Døskeland, A. Martinez, P.M. Knappskog, T. Flatmark, Phosphorylation of recombinant human phenylalanine hydroxylase: effect on catalytic activity, substrate activation and protection against non-specific cleavage of the fusion protein by restriction protease, Biochem. J. 313 (Pt 2) (1996) 409–414.

[22] U.K. Laemmli, Cleavage of structural proteins during the assembly of the head of bacteriophage T4, Nature 227 (1970) 680–685.

[23] R. Eisert, L. Felau, L.R. Brown, Methods for enhancing the accuracy and reproducibility of Congo red and thioflavin T assays, Anal. Biochem. 353 (2006) 144–146.

[24] I. Aukrust, L. Evensen, H. Hollås, F. Berven, R.A. Atkinson, G. Travé, T. Flatmark, A. Vedeler, Engineering, biophysical characterisation and binding properties of a soluble mutant form of annexin A2 domain IV that adopts a partially folded conformation, J. Mol. Biol. 363 (2006) 469–481.

[25] A.P. Døskeland, S.O. Døskeland, D. Øgreid, T. Flatmark, The effect of ligands of phenylalanine 4-monooxygenase on the cAMP-dependent phosphorylation of the enzyme, J. Biol. Chem. 259 (1984) 11242–11248.

[26] V.J. LiCata, N.M. Allewell, Is substrate inhibition a consequence of allostery in aspartate transcarbamylase? Biophys. Chem. 64 (1997) 225–234.

[27] T. Solstad, T. Flatmark, Microheterogeneity of recombinant human phenylalanine hydroxylase as a result of nonenzymatic deamidations of labile amide containing amino acids. Effects on catalytic and stability properties, Eur. J. Biochem. 267 (2000) 6302–6310.

[28] V. Parthiban, M.M. Gromiha, D. Schomburg, CUPSAT: prediction of protein stability upon point mutations, Nucleic Acids Res. 34 (2006) W239–W242.

[29] A. Benedix, C.M. Becker, B.L. de Groot, A. Caflisch, R.A. Böckmann, Predicting free energy changes using structural ensembles, Nat. Methods 6 (2009) 3–4.

[30] E. Lacroix, A.R. Viguera, L. Serrano, Elucidating the folding problem of alpha-helices: local motifs, long-range electrostatics, ionic-strength dependence and prediction of NMR parameters, J. Mol. Biol. 284 (1998) 173–191.

[31] S.C. Flores, K.S. Keating, J. Painter, F. Morcos, K. Nguyen, E.A. Merritt, L.A. Kuhn, M.B. Gerstein, HingeMaster: normal mode hinge prediction approach and integration of complementary predictors, Proteins 73 (2008) 299–319.

[32] H. Erlandsen, F. Fusetti, A. Martinez, E. Hough, T. Flatmark, R.C. Stevens, Crystal structure of the catalytic domain of human phenylalanine hydroxylase reveals the structural basis for phenylketonuria, Nat. Struct. Biol. 4 (1997) 995–1000.

[33] F. Fusetti, H. Erlandsen, T. Flatmark, R.C. Stevens, Structure of tetrameric human phenylalanine hydroxylase and its implications for phenylketonuria, J. Biol. Chem. 273 (1998) 16962–16967.

[34] B. Kobe, I.G. Jennings, C.M. House, B.J. Michell, K.E. Goodwill, B.D. Santarsiero, R.C. Stevens, R.G. Cotton, B.E. Kemp, Structural basis of autoregulation of phenylalanine hydroxylase, Nat. Struct. Biol. 6 (1999) 442–448.

[35] K.T. O'Neil, W.F. DeGrado, A thermodynamic scale for the helix-forming tendencies of the commonly occurring amino acids, Science 250 (1990) 646–651.

[36] C.G. Evans, S. Wisen, J.E. Gestwicki, Heat shock proteins 70 and 90 inhibit early stages of amyloid beta-(1–42) aggregation in vitro, J. Biol. Chem. 281 (2006) 33182–33191.

[37] T. Solstad, A.J. Stokka, O.A. Andersen, T. Flatmark, Studies on the regulatory properties of the pterin cofactor and dopamine bound at the active site of human phenylalanine hydroxylase, Eur. J. Biochem. 270 (2003) 981–990.

[38] C. Aguado, B. Perez, M. Ugarte, L.R. Desviat, Analysis of the effect of tetrahydrobiopterin on PAH gene expression in hepatoma cells, FEBS Lett. 580 (2006) 1697–1701.

[39] B. Perez, L.R. Desviat, P. Gomez-Puertas, A. Martinez, R.C. Stevens, M. Ugarte, Kinetic and stability analysis of PKU mutations identified in BH4-responsive patients, Mol. Genet. Metab. 86 (Suppl 1) (2005) S11–S16.

[40] C.R. Scriver, The PAH gene, phenylketonuria, and a paradigm shift, Hum. Mutat. 28 (2007) 831–845.

[41] A.L. Pey, M. Ying, N. Cremades, A. Velazquez-Campoy, T. Scherer, B. Thöny, J. Sancho, A. Martinez, Identification of pharmacological chaperones as potential therapeutic agents to treat phenylketonuria, J. Clin. Invest. 118 (2008) 2858–2867.

[42] P. Leandro, C.M. Gomes, Protein misfolding in conformational disorders: rescue of folding defects and chemical chaperoning, Mini Rev. Med. Chem. 8 (2008) 901–911.

[43] A. Martinez, A.C. Calvo, K. Teigen, A.L. Pey, Rescuing proteins of low kinetic stability by chaperones and natural ligands phenylketonuria, a case study, Prog. Mol. Biol. Transl. Sci. 83 (2008) 89–134.

[44] G.V. Semisotnov, N.A. Rodionova, O.I. Razgulyaev, V.N. Uversky, A.F. Gripas, R.I. Gilmanshin, Study of the "molten globule" intermediate state in protein folding by a hydrophobic fluorescent probe, Biopolymers 31 (1991) 119–128.

[45] G.W. Dykes, R.H. Crepeau, S.J. Edelstein, Three-dimensional reconstruction of the 14-filament fibers of hemoglobin S, J. Mol. Biol. 130 (1979) 451–472.

[46] S. Kure, D.C. Hou, T. Ohura, H. Iwamoto, S. Suzuki, N. Sugiyama, O. Sakamoto, K. Fujii, Y. Matsubara, K. Narisawa, Tetrahydrobiopterin-responsive phenylalanine hydroxylase deficiency, J. Pediatr. 135 (1999) 375–378.

[47] M.D. Boveda, M.L. Couce, D.E. Castineiras, J.A. Cocho, B. Perez, M. Ugarte, J.M. Fraga, The tetrahydrobiopterin loading test in 36 patients with hyperphenylalaninaemia: evaluation of response and subsequent treatment, J. Inherit. Metab. Dis. 30 (2007) 812.

[48] M.R. Zurfluh, J. Zschocke, M. Lindner, F. Feillet, C. Chery, A. Burlina, R.C. Stevens, B. Thöny, N. Blau, Molecular genetics of tetrahydrobiopterin-responsive phenylalanine hydroxylase deficiency, Hum. Mutat. 29 (2008) 167–175.

[49] P. Leandro, M.C. Lechner, I. Tavares de Almeida, D. Konecki, Glycerol increases the yield and activity of human phenylalanine hydroxylase mutant enzymes produced in a prokaryotic expression system, Mol. Genet. Metab. 73 (2001) 173–178.

[50] C. Nascimento, J. Leandro, I. Tavares de Almeida, P. Leandro, Modulation of the activity of newly synthesized human phenylalanine hydroxylase mutant proteins by low-molecular-weight compounds, Protein J. 27 (2008) 392–400.

[51] J.L. Song, D.T. Chuang, Natural osmolyte trimethylamine N-oxide corrects assembly defects of mutant branched-chain alpha-ketoacid decarboxylase in maple syrup urine disease, J. Biol. Chem. 276 (2001) 40241–40246.

[52] V.N. Uversky, J. Li, A.L. Fink, Trimethylamine-N-oxide-induced folding of alpha-synuclein, FEBS Lett. 509 (2001) 31–35.

[53] D.S. Yang, C.M. Yip, T.H. Huang, A. Chakrabartty, P.E. Fraser, Manipulating the amyloid-beta aggregation pathway with chemical chaperones, J. Biol. Chem. 274 (1999) 32970–32974.

[54] D.E. Ehrnhoefer, J. Bieschke, A. Boeddrich, M. Herbst, L. Masino, R. Lurz, S. Engemann, A. Pastore, E.E. Wanker, EGCG redirects amyloidogenic polypeptides into unstructured, off-pathway oligomers, Nat. Struct. Mol. Biol. 15 (2008) 558–566.

[55] R. Khurana, C. Coleman, C. Ionescu-Zanetti, S.A. Carter, V. Krishna, R.K. Grover, R. Roy, S. Singh, Mechanism of thioflavin T binding to amyloid fibrils, J. Struct. Biol. 151 (2005) 229–238.

[56] M.I. Ivanova, M.J. Thompson, D. Eisenberg, A systematic screen of beta(2)-microglobulin and insulin for amyloid-like segments, Proc. Natl. Acad. Sci. U. S. A. 103 (2006) 4079–4082.

[57] M.J. Bennett, M.R. Sawaya, D. Eisenberg, Deposition diseases and 3D domain swapping, Structure 14 (2006) 811–824.

[58] F.A. Ferrone, J. Hofrichter, W.A. Eaton, Kinetics of sickle hemoglobin polymerization. I. Studies using temperature-jump and laser photolysis techniques, J. Mol. Biol. 183 (1985) 591–610.

[59] G. Dykes, R.H. Crepeau, S.J. Edelstein, Three-dimensional reconstruction of the fibres of sickle cell haemoglobin, Nature 272 (1978) 506–510.

[60] A.J. Stokka, R.N. Carvalho, J.F. Barroso, T. Flatmark, Probing the role of crystallographically defined/predicted hinge-bending regions in the substrate-induced global conformational transition and catalytic activation of human phenylalanine hydroxylase by single-site mutagenesis, J. Biol. Chem. 279 (2004) 26571–26580.

[61] M. Thorolfsson, B. Ibarra-Molero, P. Fojan, S.B. Petersen, J.M. Sanchez-Ruiz, A. Martinez, L-phenylalanine binding and domain organization in human phenylalanine hydroxylase: a differential scanning calorimetry study, Biochemistry 41 (2002) 7573–7585.

[62] A.M. Fernandez-Escamilla, F. Rousseau, J. Schymkowitz, L. Serrano, Prediction of sequence-dependent and mutational effects on the aggregation of peptides and proteins, Nat. Biotechnol. 22 (2004) 1302–1306.

[63] T. Solstad, R.N. Carvalho, O.A. Andersen, D. Waidelich, T. Flatmark, Deamidation of labile asparagine residues in the autoregulatory sequence of human phenylalanine hydroxylase, Eur. J. Biochem. 270 (2003) 929–938.

[64] A.L. Pey, A. Martinez, The activity of wild-type and mutant phenylalanine hydroxylase and its regulation by phenylalanine and tetrahydrobiopterin at physiological and pathological concentrations: an isothermal titration calorimetry study, Mol. Genet. Metab. 86 (Suppl 1) (2005) S43–S53.

[65] A.K. Buell, G.G. Tartaglia, N.R. Birkett, C.A. Waudby, M. Vendruscolo, X. Salvatella, M.E. Welland, C.M. Dobson, T.P. Knowles, Position-dependent electrostatic protection against protein aggregation, Chembiochem 10 (2009) 1309–1312.

[66] F. Chiti, M. Stefani, N. Taddei, G. Ramponi, C.M. Dobson, Rationalization of the effects of mutations on peptide and protein aggregation rates, Nature 424 (2003) 805–808.

[67] K.F. DuBay, A.P. Pawar, F. Chiti, J. Zurdo, C.M. Dobson, M. Vendruscolo, Prediction of the absolute aggregation rates of amyloidogenic polypeptide chains, J. Mol. Biol. 341 (2004) 1317–1326.

[68] A. Gamez, B. Perez, M. Ugarte, L.R. Desviat, Expression analysis of phenylketonuria mutations. Effect on folding and stability of the phenylalanine hydroxylase protein, J. Biol. Chem. 275 (2000) 29737–29742.

[69] A.L. Pey, L.R. Desviat, A. Gamez, M. Ugarte, B. Perez, Phenylketonuria: genotype–phenotype correlations based on expression analysis of structural and functional mutations in PAH, Hum. Mutat. 21 (2003) 370–378.

[70] A.P. Døskeland, T. Flatmark, Conjugation of phenylalanine hydroxylase with polyubiquitin chains catalysed by rat liver enzymes, Biochim. Biophys. Acta 1547 (2001) 379–386.

[71] R.E. Baker, R. Shiman, Measurement of phenylalanine hydroxylase turnover in cultured hepatoma cells, J. Biol. Chem. 254 (1979) 9633–9639.

[72] J. Kopitz, G.O. Kisen, P.B. Gordon, P. Bohley, P.O. Seglen, Nonselective autophagy of cytosolic enzymes by isolated rat hepatocytes, J. Cell Biol. 111 (1990) 941–953.

[73] V. Kirkin, D.G. McEwan, I. Novak, I. Dikic, A role for ubiquitin in selective autophagy, Mol. Cell 34 (2009) 259–269.

[74] R. Kleppe, K. Uhlemann, P.M. Knappskog, J. Haavik, Urea-induced denaturation of human phenylalanine hydroxylase, J. Biol. Chem. 274 (1999) 33251–33258.

[75] J. Leandro, C. Nascimento, I.T. de Almeida, P. Leandro, Co-expression of different subunits of human phenylalanine hydroxylase: evidence of negative interallelic complementation, Biochim. Biophys. Acta 1762 (2006) 544–550.

[76] P.J. Kraulis, Molscript — a program to produce both detailed and schematic plots of protein structures, J. Appl. Crystallogr. 24 (1991) 946–950.

[77] W.L. Delano, The PyMOL Molecular Graphics System, DeLano Scientific, San Carlos, USA, 2002.